Loudspeaker Nonlinearities – Causes, Parameters, Symptoms

Wolfgang Klippel, Klippel GmbH, Dresden, Germany, klippel@klippel.de

ABSTRACT

This paper addresses the relationship between nonlinear distortion measurements and nonlinearities which are the physical causes for signal distortion in loudspeakers, headphones, micro-speakers and other transducers. Using simulation techniques characteristic symptoms are identified for each nonlinearity and presented systematically in a guide for loudspeaker diagnostics. This information is important for understanding the implications of nonlinear parameters and for performing measurements which describe the loudspeaker more comprehensively. The practical application of the new techniques are demonstrated on three different loudspeakers.

1. INTRODUCTION

Loudspeakers and other kinds of actuators which produce sound or vibrations behave differently at small and high amplitudes. The dependency on the amplitude is an indication of nonlinearities inherent in the system. A second nonlinear effect is the generation of additional spectral components which are not in the exciting stimulus. Those components are generally integer multiples of the applied fundamentals and thus labeled as harmonic and intermodulation distortion. The results of those distortion measurements highly depends on the properties of the stimulus such as the selected frequency, amplitude and phase of the exciting tones. The results do not completely describe the large signal performance but should be understood as symptoms. This is the major difference to the small signal domain measurement results where a linear transfer function or impulse response describes the input/output relationship completely.

Measurements which rely on symptoms are problematic because they raise following questions:
Does the measurement technique activate and detect significant symptoms of the loudspeaker nonlinearity ?
Are the symptoms meaningful ?
How are they related to the physical causes ?
How can we keep the measurement time and effort low while ensuring a comprehensive set of data ?

These questions will be addressed in the following paper. Answers will be derived from loudspeaker modeling and practical measurement results. First, the basic nonlinear mechanisms in loudspeakers are discussed. Next, traditional and new measurement techniques are summarized. After discussing general symptoms and their relationship with the nonlinear curve shape, the particular symptoms of dominant nonlinearities in loudspeakers are discussed systematically. A simple guide for assessing the large signal performance of loudspeakers is presented. This guide is then applied to diagnose three loudspeakers intended for home and automotive applications. Finally, conclusions are drawn for practical work and further research.

2. GLOSSARY OF SYMBOLS

AMD   amplitude modulation distortion in percent

Bl(x)   is the effective instantaneous electro-dynamic coupling factor (force factor of the motor) defined by the integral of the permanent magnetic flux density B over voice coil length l.

C   amplitude compression of the fundamental in dB

E   envelope of a time signal

ETHD   equivalent total harmonic distortion at the transducer's terminals in percent

EHD_n equivalent nth-order harmonic distortion at the transducer's terminals in percent

f_s resonance frequency

f_p Helmholtz resonance of the port in vented systems

FT   Fourier transform

$F_m(x,I)$ electro-magnetic driving force (reluctance force) due to the variation of the inductance versus x,

HD_n nth-order harmonic distortion in percent

H(jω)   linear transfer function

ICHD   instantaneous crest factor of harmonic distortion in dB

IHD   instantaneous value of harmonic distortion component in percent

IMD_n nth-order intermodulation distortion in percent

IMD_{total} total harmonic intermodulation distortion in percent

$i(t)$	the electric input current,
$K_{ms}(x)$	mechanical stiffness of driver suspension which is the inverse of the compliance $C_{ms}(x)$,
$L_e(x,i)$ $L_2(x,i)$ $R_2(x,i)$	lumped parameters depending on displacement x and current i required to model the para-inductance of the voice coil ,
L_{AMD}	amplitude modulation distortion in decibel
$L_{HD,n}$	nth-order harmonic distortion in the sound pressure output signal in decibel
L_{THD}	total harmonic distortion in the sound pressure output in decibel
$L_{EHD,n}$	equivalent nth-order harmonic distortion in decibel
L_{ETHD}	equivalent total harmonic distortion in decibel
L_{THD}	equivalent total harmonic distortion in decibel
$L_{IMD,n}$	nth-order intermodulation distortion in the sound pressure output signal in decibel
$L_{IMD,total}$	total harmonic intermodulation distortion in the sound pressure output signal in decibel

M_{ms} mechanical mass of driver diaphragm assembly including voice-coil and air load,

$p(t)$ sound pressure output

$P(j\omega)$ spectrum of sound pressure signal

P_n nth-order harmonic component in sound pressure

P_t rms-value of the total sound pressure signal

$P_r(f_1,U_i)$ relative amplitude of the fundamental (referred to a voltage U_i)

n order of the distortion component

R_{ms} mechanical resistance of driver suspension losses,

$R_e(T_V)$ DC resistance of voice coil,

THD total harmonic distortion in the sound pressure output in percent

$u(t)$ the driving voltage at loudspeaker terminals.

$u_D(t)$ equivalent input distortion considering all nonlinearities

$u'(t)$ total equivalent input voltage $u'=u+u_D$

$v(t)$ velocity of the voice coil,
$x(t)$ displacement of the voice coil,
$Z_m(s)$ mechanical impedance representing mechanical or acoustical load.

3. LOUDSPEAKER MODELING

At higher amplitudes all loudspeakers behave more or less nonlinearly generating signal components which do not exist in the input signal. There is a wide variety of nonlinear mechanisms occurring in loudspeaker systems and the research is mainly is focused on the "dominant nonlinearities" which

- limit acoustical output
- generate audible distortion
- indicate an overload situation
- cause unstable behavior
- are related to cost, weight, volume

- determine transducer efficiency
- affect loudspeaker system alignment.

3.1. Regular Nonlinearities

Most of the dominant nonlinearities are caused by the transducer principle and are directly related with the geometry and material properties of the motor, suspension, cone and enclosure. Physical limits require a compromise but some of the nonlinearities are also intentionally made to get a desired large signal behavior (e.g. progressive stiffness). Thus, the design process yields transducers having regular nonlinearities which are found in any good unit passing the end-of-line test.

The most dominant regular nonlinearities found in woofers, tweeters, micro-speakers, horn compression drivers and loudspeaker systems are summarized in Table 1 and discussed in the following sections.

NONLINEARITY	EFFECT	MULTIPLIED TIME SIGNALS
Stiffness $K_{ms}(x)$ of the suspension	nonlinear restoring force $F_s=K_{ms}(x)x$	displacement x
Force factor $Bl(x)$	driving force $F=Bl(x)i$ causes parametric excitation	displacement x current i
	back EMF $u_{EMF}=Bl(x)v$ causes nonlinear damping	displacement x velocity v
Inductance $L_e(x)$ (magnetic ac-field varies with coil position)	time derivative of magnetic flux $\Phi_x=L(x)i$ produces back-induced voltage	displacement x current i
	additional reluctance force $F_m \sim i^2$ driving the mechanical system	current i
Inductance $L_e(i)$ (magnetic ac-field changes permeability of the magnetic circuit)	time derivative of magnetic flux $\Phi_i=L(i)i$ produces back-induced voltage	current i
Young's modulus $E(\varepsilon)$ of the material (cone, surround)	stress in the material σ $=E(\varepsilon)\varepsilon$ is a nonlinear function of strain	strain ε
geometrical transfer matrix	geometry is changed by	strain vector ε

	mechanical vibration	
Flow resistance $R_p(v)$ of the port in vented cabinets	sound pressure inside the box is a nonlinear function of the air flow	air velocity v in the port
Doppler Effect (variation of the cone position)	variable time shift $\tau = x/c$ in the propagated signal causes phase distortion	displacement x (velocity v) sound pressure p
Nonlinear sound propagation	speed of sound $c(p)$ depends on pressure and causes wave steepening	sound pressure p

Table 1 Overview of important regular nonlinearities in an electro-dynamic loudspeaker
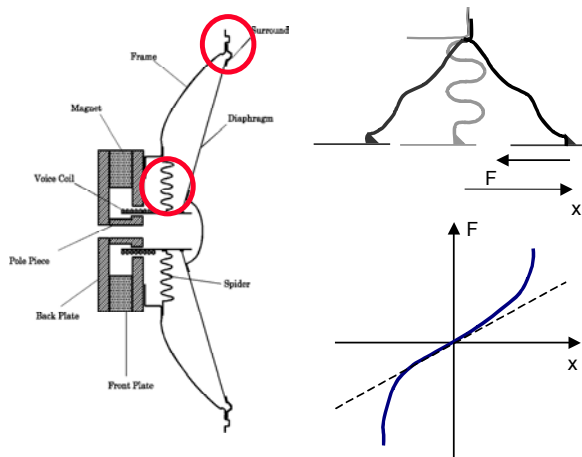
Figure 1: Suspension system in a conventional loudspeaker (sectional view) and the nonlinear force-deflection curve.

3.1.1. Nonlinear stiffness

Loudspeakers use a suspension system to center the coil in gap and to generate a restoring force which moves the coil back to the rest position. Woofers usually have a suspension comprising a spider and a surround as shown in Figure 1 which allows movements in one direction only and suppresses rocking modes.
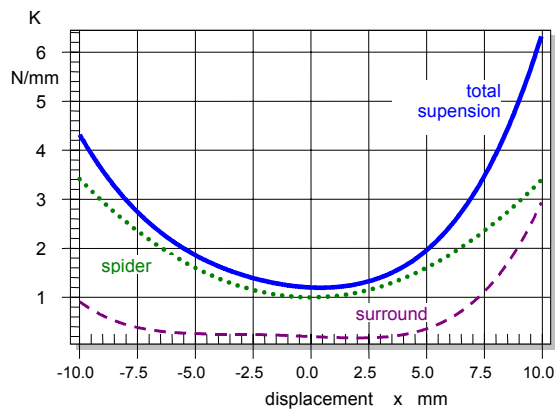
Figure 2: Stiffness of a progressive spider (dotted curve), a limiting surround (dashed curve) and the total suspension (solid curve)

Most suspension components are made of impregnated fabric, rubber or plastic molded into a particular shape. The suspension behaves like a normal spring and may be characterized by the force-deflection curve as shown in Figure 1. There is an almost linear relationship at low displacement but at high displacement the suspension responds with more force than predicted by a linear spring. In response to a slow ac-force the displacement generally follows with a hysteresis caused by losses in the material.

The restoring force $F=K_{ms}(x)x$ may also be described as the product of displacement and nonlinear stiffness $K_{ms}(x)$. The stiffness $K_{ms}(x)$ corresponds with the secant between any point of the force-reflection curve and the origin. Since the stiffness is not constant but itself a function of the displacement x, the restoring force contains products of voice coil displacement. These terms produce nonlinear distortion in the time signal which are typical for the suspension. The stiffness also varies with frequency due to the visco-elastic behavior of the suspension material. However, this effect can be modeled by a linear systems [24].

Figure 2 shows the $K_{ms}(x)$-characteristic of a spider with a progressive characteristic and a surround which limits the excursion at positive displacement.
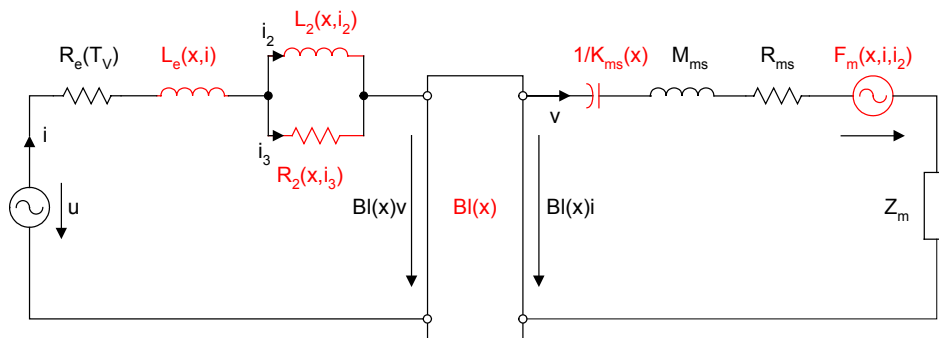
Figure 3: Electrical equivalent circuit of the loudspeaker considering motor and suspension system

3.1.2. Force Factor

The force factor *Bl(x)* describes the coupling between mechanical and electrical side of lumped parameter model of an electro-dynamical transducer as shown in Figure 3. This parameter is the integral of the flux density *B* versus voice coil wire length *l*. The force factor *Bl(x)* is not a constant but depends on the displacement *x* of the voice coil. Clearly, if the coil windings leave the gap the force factor decreases. The nonlinear function is static (no frequency dependency) and can be represented as a nonlinear graph, table or power series expansion.

The shape of the *Bl(x)*-curve depends on the geometry of the coil-gap configuration and the *B*-field generated by the magnet. Figure 4 illustrates an overhang configuration where the coil height h_{coil} is larger than depth h_{gap} of the gap. The corresponding *Bl(x)*-curve is shown as a solid line in Figure 5. For small displacements the force factor value is almost constant because the same number of windings is in the gap. A coil height equal with the gap depth corresponds with the dashed curve in Figure 5 showing a force factor that decreases without a constant region at low amplitudes.
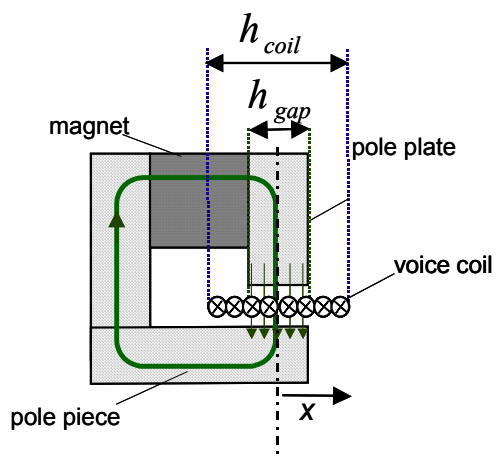
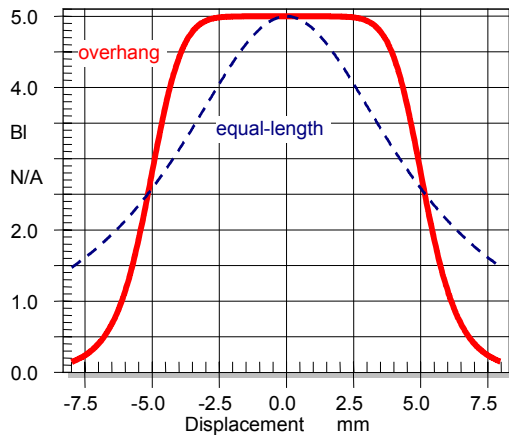Figure 4: Motor structure of a of an overhang configuration

Figure 5: Force factor *Bl(x)* of an overhang and equal-length coil-gap configuration

The force factor *Bl(x)* has two nonlinear effects as listed in Table 1:

- As a coupling factor between electrical and mechanical domain any variation of *Bl(x)* will affect the electro-dynamic driving force *F=Bl(x)i*. This mechanism is also called parametric excitation of a resonating system. High values of displacement *x* and current *i* are required to produce significant distortion.
- The second effect of *Bl(x)* is the displacement dependency of the back *EMF* generated by the movement of the coil in permanent field. Here, the force factor *Bl(x)^2* is multiplied with the velocity and causes variation of the electrical damping.

3.1.3. Voice coil inductance

The electrical input impedance depends on the position of the coil. For example, Figure 6 shows the electrical input impedance versus frequency measured at three voice coil positions (x=0, clamped at +7 mm and −7 mm). Above the resonance at 70 Hz (which does not appear for a clamped voice coil) the electrical impedance is significantly higher for a negative displacement (coil in position) than at positive displacement (coil out position).
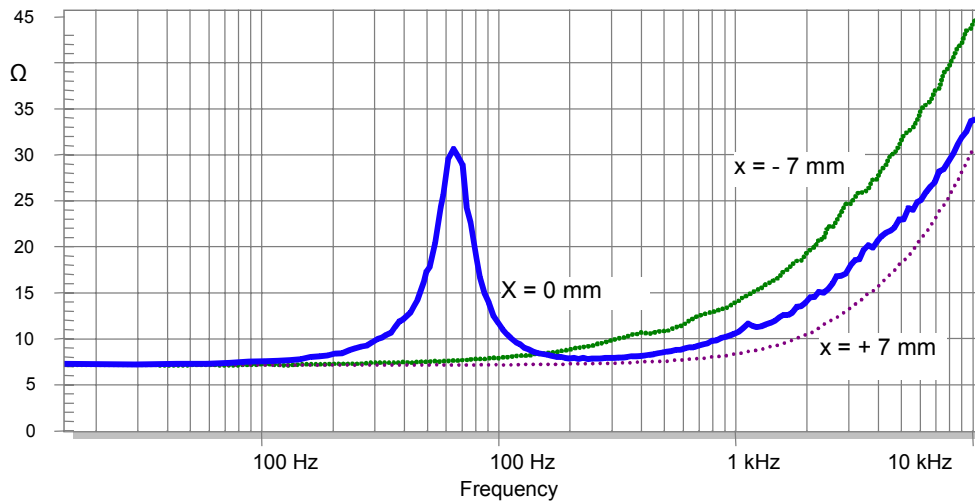
Figure 6: Electrical impedance measured at the rest position *(x=0)* and with clamped voice coil at positive and negative displacement.

This property can be observed on many loudspeakers and can be explained by the displacement-varying inductance. The current in the voice coil produces a magnetic ac-field penetrating the magnet, iron and air as shown in Figure 7. The magnetic flux depends on the position of the coil and the magnitude of the current. If the coil is in free air above the gap the inductance is much lower than when operating the coil below the gap where the surrounding material is steel which decreases the magnetic resistance.
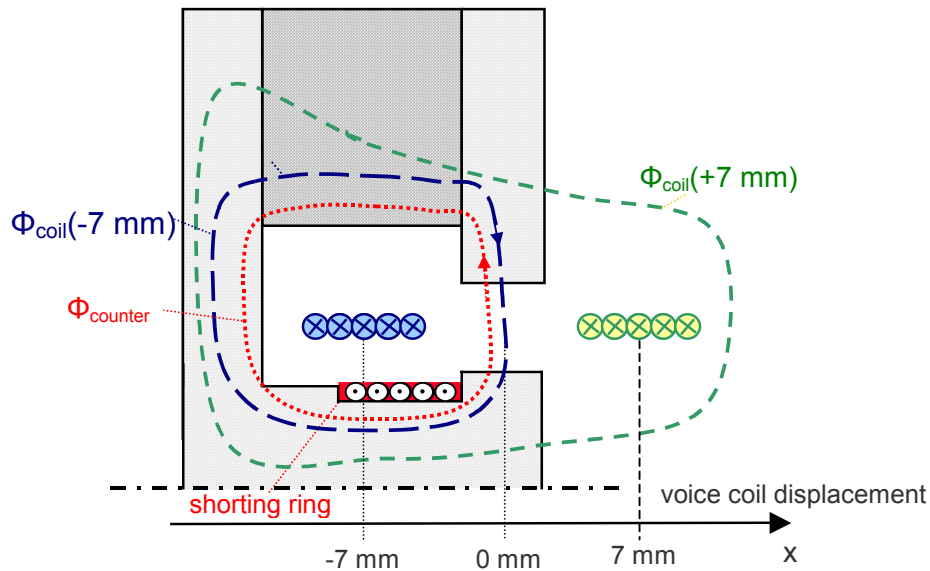
Figure 7: Motor structure of a conventional driver using a shorting ring on the pole piece.

In addition to its dependence on displacement x the inductance also depends on the input current i. This is caused by the nonlinear relationship between magnetic field strength H and flux density (induction) $B=\mu(i)H$ as shown in Figure 8. With no current applied to the coil, the permanent magnet produces the field strength H_2 which determines the working point in the $B(H)$-characteristic. A high positive current ($i = 10$ A) increases the total field strength to H_3 where the iron is more saturated and the permeability μ is decreased. Conversely, at negative current ($i = -10$ A) the total field strength is decreased, increasing the value of μ. The effect of the varying permeability $\mu.(i)$, which is very dependent on the specific magnetic material., is also called "flux modulation". The ac current also generates a hysteresis loop which corresponds with the losses in the iron material during one period of a sinusoidal current.
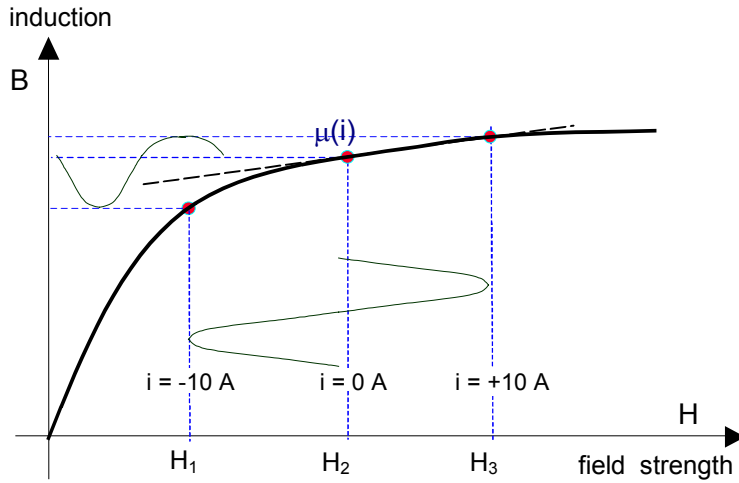
Figure 8: Flux density *B* versus magnetic field strength *H* of the magnetic circuit showing that the permeability *μ(i)* depends on the voice coil current *i*.

The magnetic ac-flux increases the impedance at higher frequencies as shown in Figure 6. This increase can not be described by an ideal inductance [2]. Special models (Leach [3], Wright [4], cascaded LR-network) are required to describe losses generated by eddy currents in the iron material. The discrete model using an inductance $L_e(x,i)$ in series with a second inductance $L_2(x,i)$ shunted by a resistor $R_2(x,i)$ as shown in Figure 3 is a good candidate for capturing the nonlinear dependence on displacement and current. The particular parameters depend on the frequency range over which the fitting is performed [5]. For most applications it is also convenient to use a simple approximation which neglects the nonlinear interactions between current and displacement. It uses the same nonlinear curve shape for the displacement-varying parameters

$$\frac{L_e(x, i = 0)}{L_e(0)} \approx \frac{L_2(x, i = 0)}{L_2(0)} \approx \frac{R_2(x, i = 0)}{R_2(0)}$$

and the current varying parameters

$$\frac{L_e(i, x = 0)}{L_e(0)} \approx \frac{L_2(i, x = 0)}{L_2(0)} \approx \frac{R_2(i, x = 0)}{R_2(0)}.$$

This approximation reduces the amount of data used in loudspeaker diagnosis and loudspeaker design calculations. The nonlinear characteristics of $L_e(x)$ versus displacement *x* and $L_e(i)$ versus i and the values $L_2(0)$ and $R_2(0)$ at the rest position *x=0* are sufficient in most applications to describe the nonlinear characteristic of the para-inductance. For example, the Figure 9 shows the relationship between $L_e(x)$ and displacement, Figure 10 shows the dependency of the $L_e(i)$ versus current, respectively.
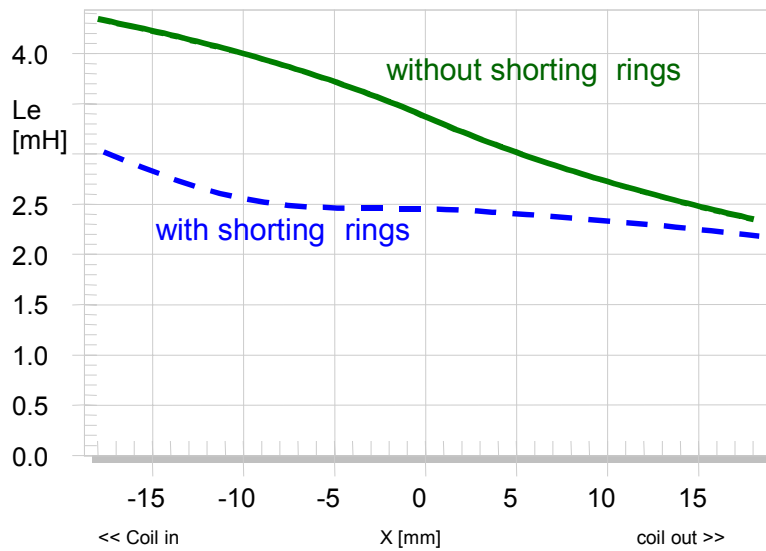
Figure 9: Voice coil inductance $L_e(x, i=0)$ versus displacement x for a motor with and without shorting rings
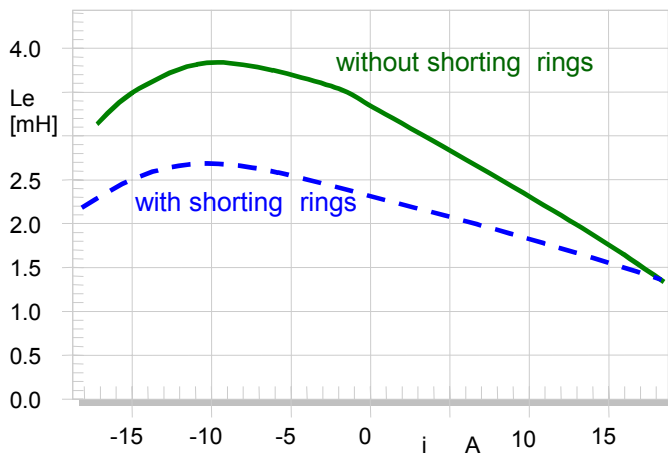

Figure 10: Voice coil inductance $L_e(i, x=0)$ versus voice coil current i with and without shorting rings

The inductance of the coil can be significantly reduced by placing conductive material (usually rings or caps made of aluminum or copper) on the pole piece or close to the coil as shown in Figure 7. The ac-field induces a current in the shorting material which generates a counter flux. This reduces the total flux and the inductance of the coil. This arrangement behaves similarly to a transformer which is shorted on the secondary side.

If the shorting material is placed at points where the inductance is maximal, the $L_e(x)$-curve can be significantly linearized as shown by the dashed line in Figure 9. Shorting materials have also a positive effect on the $L_e(i)$-characteristic because the ac-field field is smaller and produces less flux modulation.

Table 1 summarizes the nonlinear effects and shows which time signals are multiplied with each other:

- The first effect of the displacement varying inductance $L_e(x)$ is the back induced voltage in the electrical input circuit due to the time derivative of the magnetic flux and leads to the variation of the input impedance with coil displacement as shown in Figure 6. This effect is expressed with a multiplication of displacement and current. The same signals are involved in the parametric excitation of the $Bl(x)$ but there is an additional differentiation after the multiplication which enhances the amplitude of the components by 6dB/octave at higher frequencies.

- The second effect is an additional reluctance force $F_m(x,i,i_2)$ which drives the mechanical system directly as shown in the equivalent circuit in Figure 3. It can be approximated by

$$F_m(x,i,i_2) \approx -\frac{i(t)^2}{2}\frac{\partial L_e(x)}{\partial x} - \frac{i_2(t)^2}{2}\frac{\partial L_2(x)}{\partial x}.$$

  The reluctance force multiplies the local derivative of $L_e(x)$ with the squared current. The squarer is the dominant nonlinear operation and generates distortion in the full audio band. The reluctance force was the major driving force in electro-magnetic loudspeaker used 50 years ago. In today's electro-dynamic transducers the reluctance force is an undesired rudiment which should be kept as low as possible.

- The dependency of $L_e(i)$ on current causes an ac-flux which depends on powers of i. Since the current is a broad band signal, distortion components are generated in the full audio band.
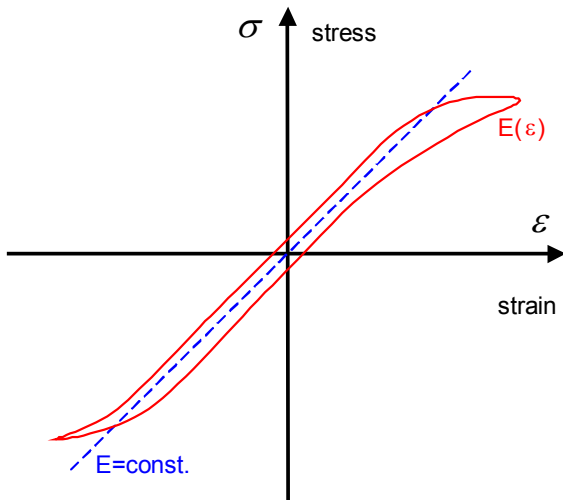
Figure 11: Nonlinear material properties as causes for nonlinearities in the mechanical system

3.1.4. Nonlinear Material properties

At low frequencies where the cone vibrates as a piston the suspension is the only nonlinear part of the mechanical system and can be described by a single lumped parameter $K_{ms}(x)$. At higher frequencies break-up modes occur on cone and other parts (voice coil former, dust cap). These vibrations become nonlinear if the strain and stress in the material is very high and Young's modulus $E(\varepsilon)$ varies with the strain ε.

Nonlinear distortion is generated in the stress σ due to the multiplication of $E(\varepsilon)$ with the strain ε, and becomes maximal at distinct frequencies (Eigenfrequencies) where the modes produce high strain in the material [6].
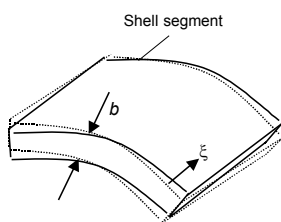

Figure 12: Variation of the cone geometry due to mechanical vibration

3.1.5. Variation of Geometry

More important than the variation of the *E*-modulus is the variation of the geometry of the mechanical system. The vibration becomes nonlinear if the displacement ζ is not small in comparison to geometrical dimensions (e.g. thickness b or curvature of the cone segment [7]) as illustrated in Figure 12.
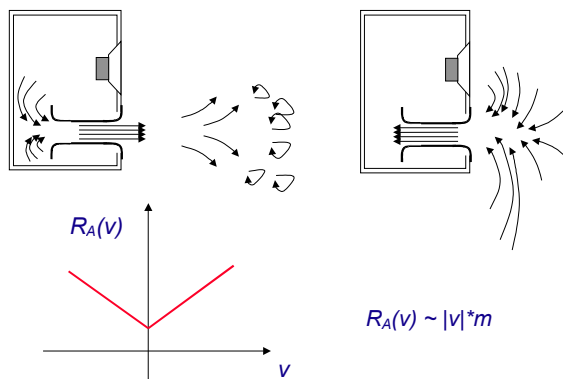

Figure 13: Nonlinear flow resistance depends on the air velocity

3.1.6. Port nonlinearity

Ports in vented systems have a flow resistance which is not constant, but highly depends on the velocity *v* of the air inside the port [8] . At very low amplitudes the loss factor of a normal port is very high ($Q > 50$) but this values goes down to 10 and less for particle velocities above 20 m/s. The reason is that the air in the port does not vibrate as an air plug where all the air particles are bounded together. During the out-breathing phase the air is pushed in axis into the far field. In the following in-breathing phase other air particles resting around the orifice are accelerated and sucked into the port. The kinetic energy moved into the far field corresponds with the increase of the flow resistance for positive and negative air velocities as illustrated in Figure 13.

The nonlinear flow resistance $R_p(v)$ generates low frequency components because the velocities are multiplied with each other. An asymmetry in $R_p(v)$ caused by the geometry of the orifices generates a dc-pressure in the box which may spoil the voice coil position and cause motor distortion.

A second nonlinear mechanism is the generation of turbulences in the air flow that behave as sound sources causing broad band noise in the output signal [9], [10] .
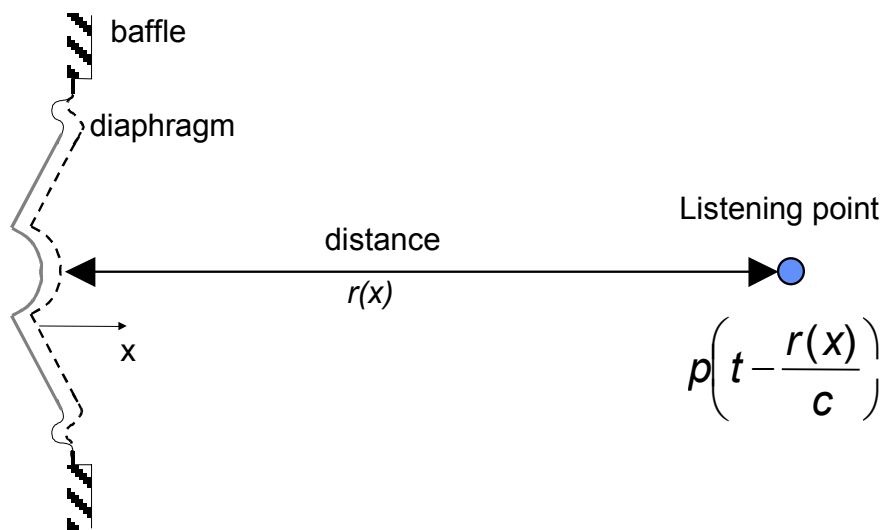
Figure 14: Phase modulation caused by varying distance between cone and listening point (Doppler Effect)

3.1.7. Doppler Effect

Variation of the position and geometry of the cone and surround does not only affect the mechanical vibration but also the acoustical radiation condition [11]. The Doppler Effect is the most dominant nonlinearity in this group. This effect may be explained as the change in wavelength as the result of motion (velocity) between source and receiver. This effect can also be described by the varying distance between the radiating surface (cone) and a listening point in axis caused by the displacement of the diaphragm generated by a low frequency component [12]. This causes a varying time delay in the transferred sound pressure signal which can be interpreted as a phase or frequency modulation . This is not very critical for the low frequency component itself but causes high intermodulation of high frequency signals with a short wavelength. This mechanism may be described by the product of displacement and differentiated sound pressure and requires low and high frequency components at the same time. The easiest way to avoid this distortion is to use a multi-way system with a sufficiently low crossover frequency between woofer and tweeter system.
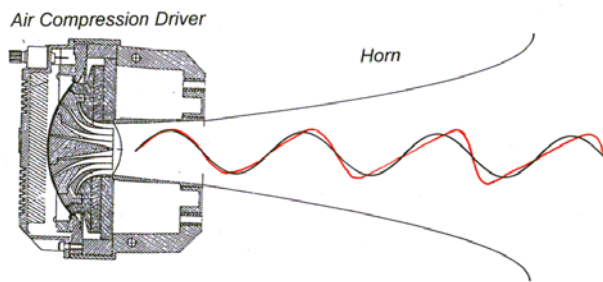
Figure 15: A sound wave propagating at high amplitudes causes a characteristic steepening of the wave front

3.1.8. Wave Steepening

At high amplitudes a sound wave propagates at the maxima faster than at the minima causing a gradual steepening of the wave front [13]. This mechanism is found in horn loaded compression drivers. The nonlinear mechanism is basically a multiplication of the sound pressure with the differentiated sound pressure in each section of the horn [14] - [16].

3.2. Irregular Defects

There are other sources of signal distortion in loudspeakers which are caused by defects such as a loose glue joint, a rubbing voice coil, a wire hitting the cone or loose particles in the gap. Usually this is also a nonlinear mechanism because the output signal contains spectral components which are not in the input *u(t)* and onset of the distortion depends highly on the amplitude of the stimulus.
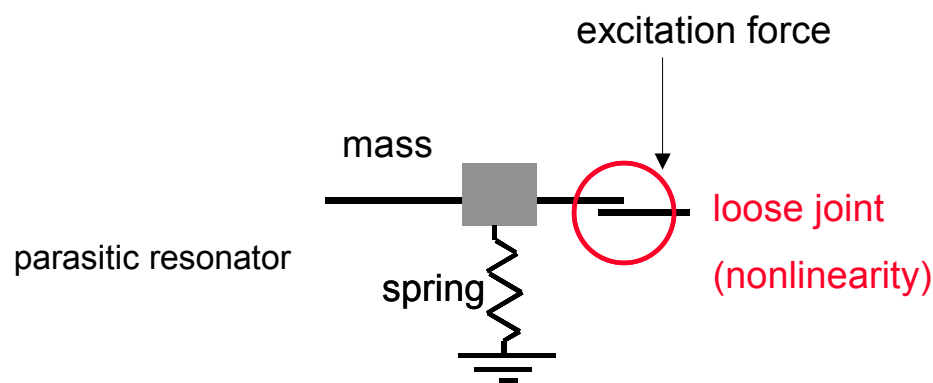

Figure 16: Mechanical model of a loudspeaker defect (glue problem)

The example in Figure 16 illustrates the effect of a defective glue joint which causes a loose connection between the outer edge of the surround and the loudspeaker frame. The loose part of the surround is modeled by lumped elements (moving mass, spring, losses) forming a resonator

with a high Q factor. The loose joint provides a nonlinear excitation which switches the driving force on and off depending on the direction of the displacement. If the joint is open, the mass-spring resonator oscillates at a resonance frequency f_o which is much higher than the exciting frequency f. The external stimulus initiates and synchronizes the oscillations and provides the required energy. Applying a sinusoidal excitation signal this system generates short bursts at certain time instances spaced periodically.

A more detailed analysis of the loose glue joint and other loudspeaker defects is not subject of this paper but are discussed elsewhere [17], [18].

3.3. Measurement of model parameters

Modeling becomes practical if the free parameters of the model can be identified on a particular unit. The parameters of the lumped parameter model in Figure 3 can be measured by using static, incremental dynamic or full dynamic techniques as defined in the IEC standard [19]. The static and the incremental dynamic methods [21], [20] use a dc-part in the stimulus to operate the loudspeaker in a particular working point. However, only a full dynamic measurement technique [22], [23] operates the loudspeaker under normal working conditions and can use an audio-signal as stimulus. This is important for considering visco-elastic effects of the suspension [24] and for measuring the inductance $L_e(i)$ at high currents (> 30 Ampere) where heating of the coil may damage the loudspeaker. In this paper all large signal parameters are measured dynamically by using the system identification technique (LSI of the Distortion Analyzer [25]).

3.4. Simulation of signal performance

If the loudspeaker model is adequate and the free parameters are measured carefully, the behavior of the loudspeaker may be predicted for any input signal (synthetic test signal or music as stimulus). This kind of lumped parameter analysis [1] has the following advantages:

The simulation does not need any sensor but gives access to all state variables of the system (sound pressure, current, displacement,..). It is also possible to separate nonlinear distortion of each nonlinearity from the linear output and to measure the magnitude of the distortion in an audio signal at any time [26]. Modeling is also the basis for a new auralization technique [27] which combines objective and subjective assessment of the large signal performance.

4. MEASUREMENT OF SYMPTOMS

The traditional method of assessing the large signal performance is the measurement of special symptoms generated by the nonlinear system at high amplitudes [28]. Such symptoms are:

- generation of new spectral components in the output signal (which can be identified as harmonic, sub-harmonic and intermodulation components)

- Nonlinear relationship between the amplitude of the input and output amplitude of fundamental and distortion components ("nonlinear amplitude compression")

- Generation of a dc-part in the state variables (e.g. dc-displacement) [30]

- Instabilities leading to bifurcation and jumping effects [29].

Those symptoms give valuable information about:

- deviation from linear behavior (almost linear, weak nonlinear or strong nonlinear behavior)

- physical nature of the nonlinearity (e.g. force factor)

- shape of the nonlinear characteristic

- quantitative identification of nonlinear parameters.

4.1. Critical stimulus

Symptoms are only generated if the nonlinearities are activated by an appropriate stimulus. Since the nonlinearities of the motor and suspension are relatively smooth curves, the loudspeaker behaves almost linearly for sufficiently small amplitudes. High displacement is required to cause significant variation of the force factor $Bl(x)$, inductance $L_e(x)$ and stiffness $K_{ms}(x)$. Therefore, the stimulus should provide sufficient energy at frequencies below $2f_s$ because the displacement decreases by 12 dB/octave above resonance frequency f_s. Detection of current-varying inductance $L_e(i)$ requires a signal which creates high voice coil current. Due to the electrical input impedance variation with frequency the current is high at low frequencies, becomes minimal at the resonance, increases to high values again at $2f_s$, and gradually decays at higher frequencies.

The nonlinear terms in Table 1 which multiply two different time signals require a stimulus which produces high amplitudes of both state variables at the same time. In some cases this can not be accomplished by a single tone. For example the L(x)-nonlinearity requires at least a low frequency tone for generating displacement and a high frequency tone for generating sufficient current. A two-tone stimulus has the advantage over a multi-tone signal in that the generated components can be separated in the frequency domain to simplify the identification and interpretation.

4.2. Monitoring of State Variables

The sound pressure output measured by a microphone is, of course, the most natural candidate for monitoring the state of the loudspeaker. However, cone vibration radiation, the room and ambient noise have an influence on the acoustic signal. Monitoring the voice coil displacement

by a triangulation laser sensor is a more direct way of observing the state of the suspension and motor. A considerable dc-component may be generated in the displacement by asymmetrical nonlinearities (rectification process). The input current is also a very informative state signal and can also be easily measured. The dynamic measurement of the large signal parameters in the LSI module [25] is based on monitoring electrical signals at the loudspeaker terminals only. Monitoring the voltage at the terminals is useful if the loudspeaker is operated via a high impedance amplifier (current source). Monitoring of velocity and cone acceleration can be accomplished by using an expensive Doppler laser system or an inexpensive accelerometer mounted on the cone.

4.3. Signal Analysis and Distortion Measures

A nonlinear system excited by a two-tone stimulus $u(t)= 1.4U_0 sin(2\pi f_1 t)+1.4U_0 sin(2\pi f_2 t)$ with a first excitation tone at frequency f_1 and a second tone at f_2 generates a state variable (e.g. sound pressure $p(t)$) which is subjected to a spectral analysis (Fourier transform FT) giving the spectrum (e.g $P(j\omega)=FT\{p(t)\}$).
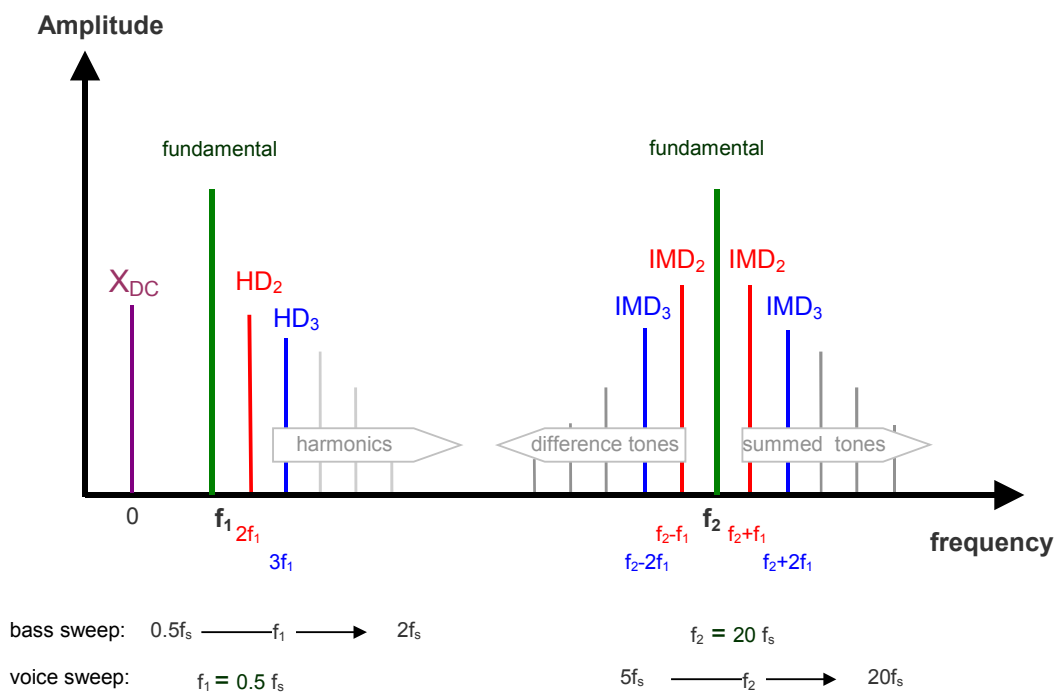
Figure 17 Spectrum of a state variable (e.g. sound pressure, displacement, current) generated by a two-tone stimulus

If the distance between the two tones is sufficiently high ($f_2 >> f_1$) the fundamental components, harmonic and intermodulation components are nicely separated and can be easily identified as illustrated in Figure 17.

4.3.1. Fundamental Components

The complex spectrum $P(j\omega)=FT\{p(t)\}$ comprises the fundamental components $P(j\omega_1)$ and $P(j\omega_2)$. While performing a series of measurements with varied frequency f_1 the amplitude and phase response of the fundamental component can be measured in the frequency range of interest. In contrast to the linear transfer response measured at sufficiently small amplitudes, the large signal response depends on the amplitude and the spectral content of the stimulus. Thus the second tone at f_2 may influence the amplitude of the output component $P(j\omega_1)$. In this paper all measurements of the fundamental components are performed with a single tone f_1.

Although the phase response changes significantly at higher amplitude it plays a minor role in loudspeaker diagnostics so far.

More important is the relationship between input and output magnitude which reveals the nonlinear amplitude compression. In practice a series of measurements $i= 1, ... N$ is performed while changing the amplitude of the input signal $U_o=i*\Delta U$ and calculating the relative amplitude

$$P_r(f_1,U_i) = \frac{|P(j2\pi f_1)|}{U_i}U_1 .$$

(1)

The measure $P_r(f_1, U_i)$ is a convenient basis for comparing all measurements in one diagram and for calculating the amplitude compression

$$C(f_1,U_i) = 20\lg\left(\frac{P_r(f_1,U_1)}{P_r(f_1,U_i)}\right).$$

(2)

4.3.2. Harmonic Distortion

The 2nd-order, 3rd-order and higher-order harmonic components $P_n(j\omega_1)=0.7P(nj\omega_1)$ with $n > 1$ appear at $2f_1$, $3f_1$ and multiples $nj\omega_1$ of the fundamental frequency f_1. The harmonics of the second tone f_2 are at higher frequencies which are not shown in Figure 17. According to the IEC standard 60268-5 [31] the nth-order **H**armonic **D**istortion may be expressed in percent

$$HD_n = \frac{|P_n|}{P_t}100$$

(3)

or in decibel

$$L_{HD,n} = 20\lg\left(\frac{HD_n}{100}\right),$$

(4)

the **T**otal **H**armonic **D**istortion in percent

$$THD = \frac{\sqrt{\sum_{i=2}^{N}|P_i|^2}}{P_t}100 \qquad (5)$$

or in decibel

$$L_{THD} = 20\lg\left(\frac{THD}{100}\right) \qquad (6)$$

using the rms-value of the total signal

$$P_t = \sqrt{\frac{1}{T}\int_0^T p(t)^2\,dt}\ . \qquad (7)$$

The common presentation methods for harmonic distortion measurement results have some disadvantages:

The measures HD_n, THD in Eqs. (3) and (5), respectively, refer the amplitude of the measured distortion components to the rms-value P_t of the total signal $p(t)$. In this way the measured distortion responses depend on the fundamental which is mainly determined by the linear transfer function $H(j\omega)$. This yields high values of harmonic distortion at low frequencies where the radiation of the harmonics is much better than the radiation of the fundamental. Also, break up modes, radiation, deflections of the sound wave at the enclosure edges and reflections in the room increase the complexity of the distortion curves [32].
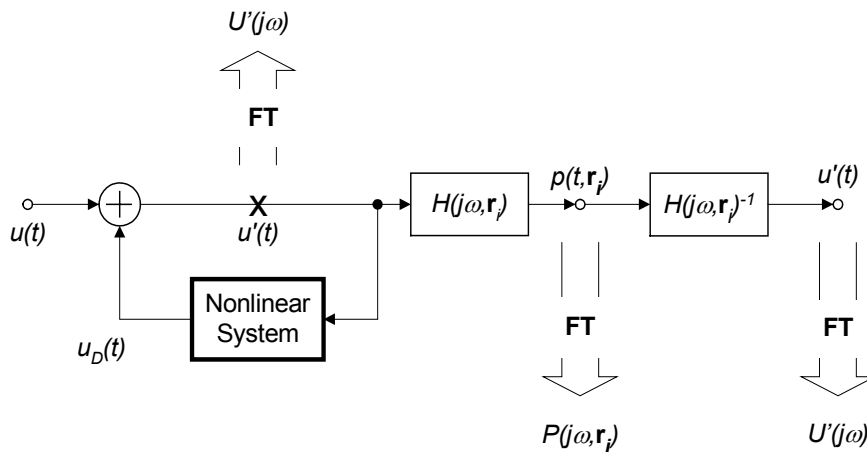
Figure 18: Measurement of equivalent input distortion by performing an inverse filtering prior to spectral analysis.

The results of the distortion measurement are much easier to interpret if the distortion is measured closer to the source. Since most of the dominant distortion is generated in the one-dimensional signal path (motor, suspension) it can be lumped together in a signal source adding

distortion $u_D(t)$ to the input signal $u(t)$ as shown in Figure 18. Unfortunately, this point is not accessible for direct measurements in real loudspeakers. However, distortion measured in sound pressure, displacement or any other state variable can easily be transformed into the input signal by filtering with the inverse transfer function $H(j\omega)^{-1}$. This concept [33] produces less, but more meaningful data and is a convenient way for separating motor distortion from distortion generated in the multi-dimensional domain (break-up modes, radiation).

The *nth*-order **E**quivalent **H**armonic **I**nput **D**istortion in percent is defined in percent

$$EHD_n = \frac{|U_n|}{U_t} 100 \quad, \quad \text{for } n > 1 \tag{8}$$

or in decibel

$$L_{EHD,n} = 20 \lg \left(\frac{EHD_n}{100} \right) ., \quad \text{for } n > 1, \tag{9}$$

the **E**quivalent **T**otal **H**armonic **I**nput **D**istortion in percent

$$ETHD = \frac{\sqrt{|U_2|^2 + |U_3|^2 + \dots |U_3|^2}}{U_t} 100 \tag{10}$$

or in decibel

$$L_{ETHD} = 20 \lg \left(\frac{ETHD}{100} \right) \tag{11}$$

using the equivalent input components

$$U_n(j\omega_1) = \frac{P_n(j\omega_1)}{H(nj\omega_1)} , n > 0 \tag{12}$$

and the rms value of the total input voltage signal U_t

$$U_t = \sqrt{\frac{1}{T} \int_0^T u(t)^2 + u_D(t)^2 \, dt} . \tag{13}$$
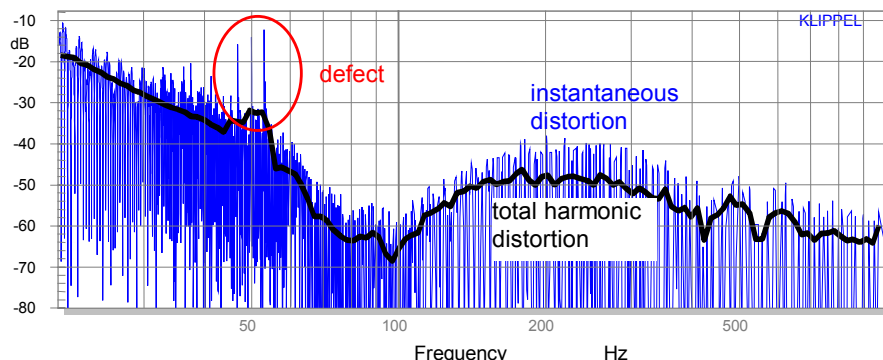
Figure 19: Instantaneous distortion IHD and total harmonic distortion THD in sound pressure output measured with a sinusoidal sweep on a defective loudspeaker.

Traditional harmonic distortion measurements only exploit the amplitude of the harmonic components. The phase of the higher-order harmonics is usually neglected because the interpretation is difficult. However, both phase and amplitude spectrum determine the waveform of the distortion in the time domain [34]. The waveform of the harmonic distortion signal can be calculated for a sinusoidal stimulus at ω by applying the inverse Fourier transform to the harmonics in the complex spectrum giving the **I**nstantaneous **H**armonic **D**istortion in percent

$$IHD(t) = \frac{\left| \sum_{i=2}^{N} P_i e^{ji\omega t} + P_i^* e^{-ji\omega t} \right|}{p(t)} 100 \qquad (14)$$

or in decibel

$$L_{IHD} = 20 \lg\left(\frac{IHD}{100}\right). \qquad (15)$$

For a sinusoidal sweep the time t corresponds with an instantaneous frequency $\omega(t)$ giving the frequency response $L_{IHD}(f)$. For example, Figure 19 shows instantaneous harmonic distortion $L_{IHD}(f)$ as thin line and the total harmonic distortion *THD* as a thick line versus frequency between 20 Hz and 1 kHz. The ratio between the instantaneous distortion (*IHD*) and the rms-value of the distortion (*THD*) gives the **I**nstantaneous **C**rest factor of **H**armonic **D**istortion

$$ICHD = 20 \lg\left(\frac{IHD}{THD}\right). \qquad (16)$$

in decibel. This measure describes the transient and impulsive properties of the harmonic distortion and plays an important role in the separation of soft- or hard limiting nonlinearities and the identification of loudspeaker defects. For example, distortion caused by regular motor and suspension nonlinearities produces relatively smooth distortion curves and the *ICHD* stays below

10 dB. A loudspeaker defect such as a wire beat generates a much higher crest factor (*ICHD* > 10 dB) as shown at 50 Hz in Figure 19.

4.3.3. Intermodulation Distortion

The IEC standard [31] summarizes the summed and difference-tone components of the same order and defines the nth-order **I**nter-**M**odulation **D**istortion (n > 1) in percent

$$IMD_n = \frac{|P(j\omega_2 - (n-1)j\omega_1)| + |P(j\omega_2 + (n-1)j\omega_1)|}{|P(j\omega_2)|} 100 \tag{17}$$

or in decibel

$$L_{IMD,n} = 20\lg\left(\frac{IMD_n}{100}\right). \tag{18}$$

Summarizing all nth-intermodulation distortion gives the **T**otal **I**nter-**M**odulation **D**istortion in percent.

$$IMD_{Total} = \sqrt{\sum_{i=2}^{N} \exp_{10}(IMD_i / 10)} \cdot 100 \tag{19}$$

or in decibel

$$L_{IMD,total} = 20\lg\left(\frac{IMD_{Total}}{100}\right). \tag{20}$$

In this paper two kinds of intermodulation distortion measurements are used:

1. Sweeping the Bass-Tone

The first tone f_1 is varied from *f$_s$/2* to *2f$_s$* and the second tone is set at the constant frequency *f$_2$=10f$_s$*.

2. Sweeping the Voice-Tone

The fist tone is set at a constant frequency $f_1=f_s/5$ and the second tone f_2 is varied from *7f$_s$* to *20f$_s$*.
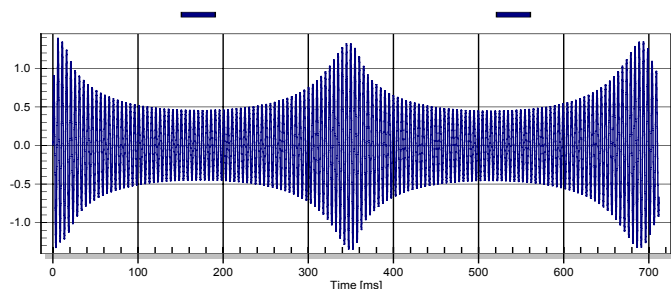
Figure 20: Amplitude modulation of a high-frequency tone by a low frequency tone caused by a nonlinear force factor *Bl(x)*
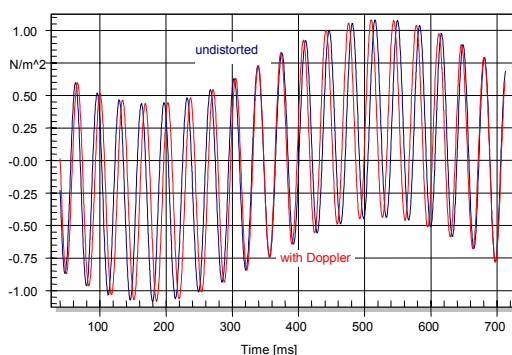
Figure 21: Phase modulation of a high-frequency tone by a low frequency tone caused by the Doppler effect

4.3.4. Separation of *FM* and *AM* Distortion

The IEC standard 60268-5 [31] and other traditional intermodulation measurements exploit the amplitude of the tones in the sidebands only. The phase of the components give further information to identify the modulation mechanism:

The **A**mplitude **M**odulation (AM) causes a variation of the envelope of the first tone (carrier) according to the modulating second tone but does not affect the phase of the carrier [35]. The parametric excitation due to the *Bl(x)* is a typical example for amplitude modulation. Figure 20 shows one period of the low frequency tone modulating the envelope of the radiated high-frequency tone.

The **F**requency **M**odulation (*FM*) does not change the envelope of the signals but changes the phase of the high frequency tone. For example, Figure 21 shows the waveforms of a radiated two-tone signal with and without Doppler effect over one period of the low frequency tone. The phase of the high frequency tone changes with the amplitude of the low frequency tone.

The intermodulation generated by an *AM*-process can be described by the **A**mplitude **M**odulation **D**istortion expressed in percent

$$AMD = \frac{\sqrt{\dfrac{2}{K}\sum_{k=1}^{K}\left(E[k]-\overline{E}\right)^2}}{\overline{E}} * 100 \tag{21}$$

or in decibel

$$L_{AMD} = 20\lg\left(\frac{AMD}{100}\right) \tag{22}$$

by using the instantaneous envelope *E[k]* and the averaged envelope

$$\overline{E} = \frac{1}{K}\sum_{k=1}^{K}E[k] \tag{23}$$

of the modulated high-frequency tone which can be calculated from complex spectrum by using the analytical signal [36].

The measures *AMD* and L_{AMD} show the contribution of amplitude modulation and can be compared with the total intermodulation measures IMD_{Total} and $L_{IMD,total}$ which consider both *FM* and *AM* distortion.

4.4. Dc-Displacement

If some of the nonlinearities have an asymmetrical shape a rectification process takes place and a dc-component X_{dc} is generated in the voice coil displacement [37]. A dc-part can not be generated in velocity, acceleration or the corresponding sound pressure output because those time signals are derivatives of the displacement. The voice coil current is also free of a dc-component because the magnetic flux is differentiated and the back-EMF is the product of two orthogonal time signals (displacement and velocity).

5. EFFECTS OF THE CURVE SHAPE

There are some general relationships between the shape of nonlinearity and the magnitude of the low- and high-order distortion components independent of the physical context and the location of the nonlinearity in the differential equation.

The following discussion uses the $K_{ms}(x)$ and Bl(x)-nonlinearities as examples.

5.1. Symmetry and asymmetry

The most obvious feature of a nonlinear parameter is the symmetry of the curve. A well-made loudspeaker should have symmetric $K_{ms}(x)$ and *Bl(x)* curves. At high positive and negative

excursion the suspension will be limited by unfolded and stretched suspension material and the voice coil will leave the gap. A symmetric curve usually produces 3rd- and other odd-order distortion components as illustrated in Table 2. No dc-displacement or other even-order distortion components are generated as long as the nonlinear system is stable. A loudspeaker may become unstable if a motor with an equal-length coil–gap configuration is combined with a soft suspension [30].
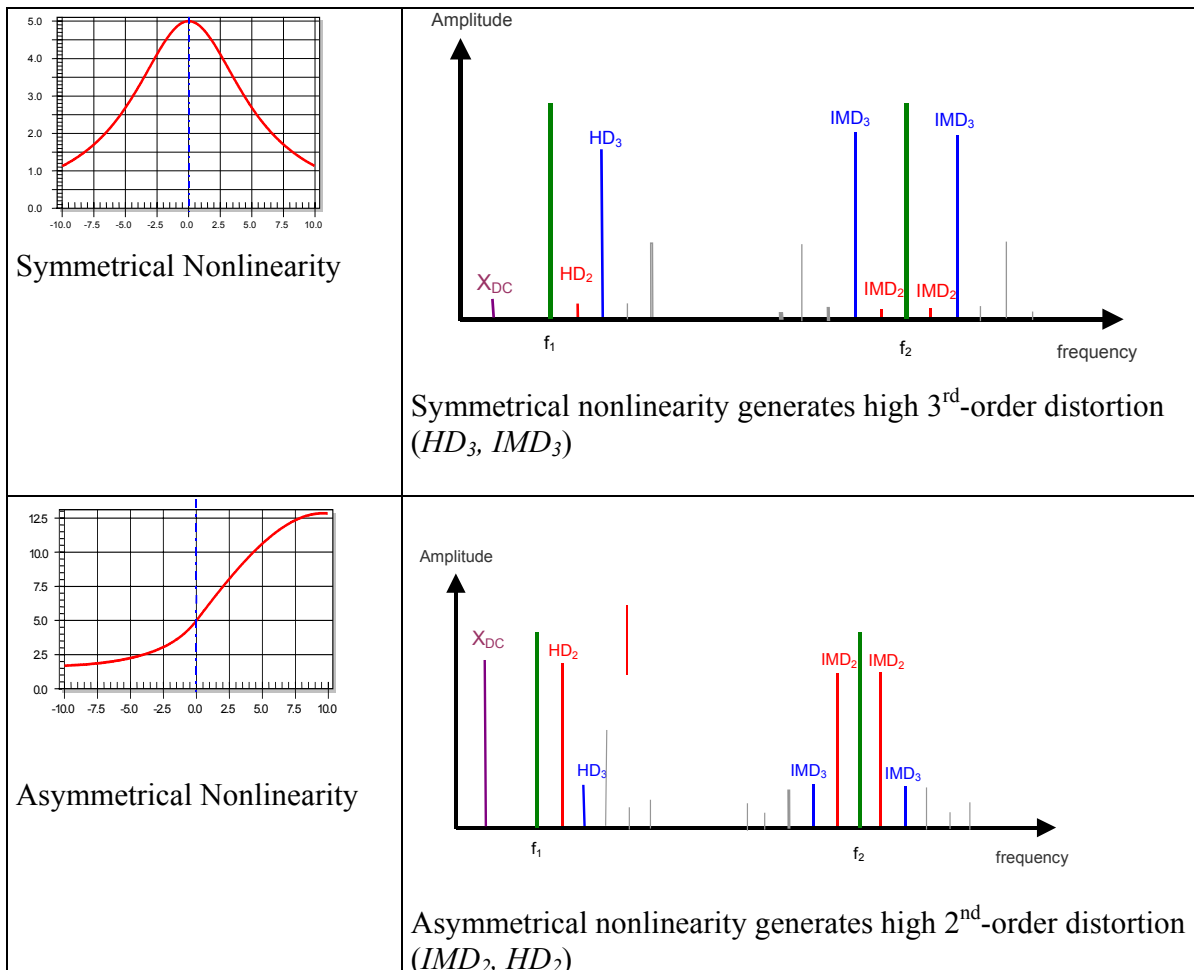
 Symmetrical Nonlinearity	 Symmetrical nonlinearity generates high 3rd-order distortion (*HD₃, IMD₃*)
 Asymmetrical Nonlinearity	 Asymmetrical nonlinearity generates high 2nd-order distortion (*IMD₂, HD₂*)

Table 2 Relationship between shape of nonlinearities and the generated odd- and even-order distortion components

Other nonlinearities, such as the inductance of a driver without shorting ring, the Doppler effect and wave steepening, have a distinct asymmetry that is difficult (inductance) or impossible (wave steepening) to eliminate. Asymmetric nonlinearities generate primarily even-order distortion. However, since these nonlinearities are usually part of a feedback loop (a characteristic of systems that can be described with a nonlinear differential equation) odd-order

distortion components are also generated by multiplying the even-order distortion with the fundamental component.

5.2. Soft- and hard-limiting nonlinearities

Another obvious feature of the nonlinear curve shape is the steepness of the curve. Motors where coil and gap have the same length become nonlinear at relatively small displacement as shown as dashed line in Figure 5. Conversely, a large voice coil overhang causes a plateau where the force factor is almost constant over a certain range as shown as solid line in Figure 5. However, when the coil leaves the gap the force factor decays at a much higher rate than the equal-length configuration. For high displacement of half the coil height ($x=+-5$ mm) both configurations give the same force factor value ($Bl = 2.5$ N/A) neglecting the influence of the fringe field. If both curves are expanded into a power series the coefficient of the quadratic term is dominant for the equal-length configuration but the overhang coil will result in a dominant higher-order coefficient.
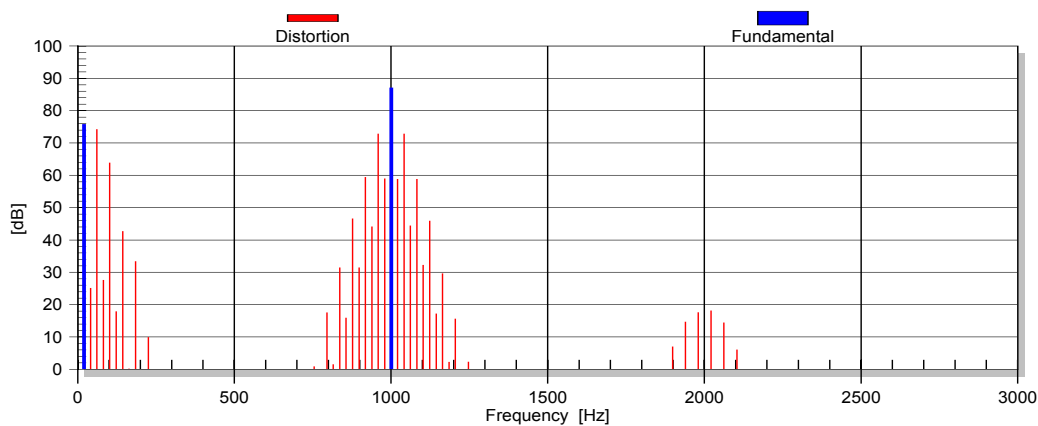
Figure 22: Spectrum of distorted two-tone stimulus in sound pressure output generated by a force factor *Bl(x)* of an equal-length coil configuration
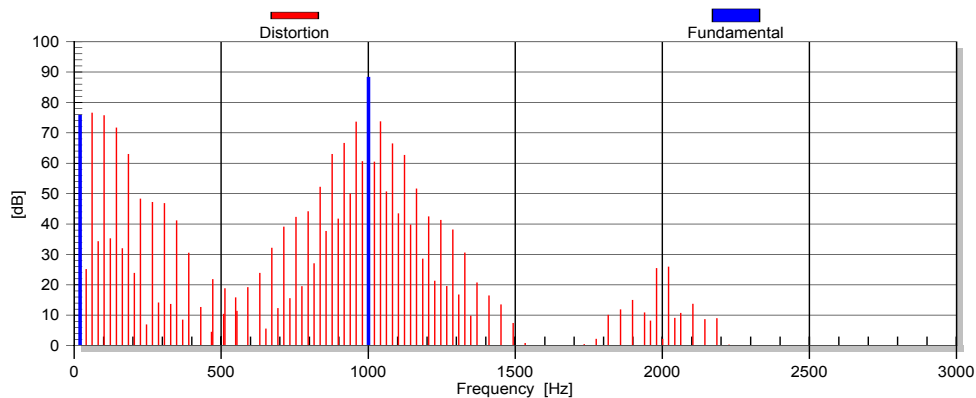
Figure 23: Spectrum of distorted two-tone stimulus in sound pressure output generated by a force factor *Bl(x)* of an overhang coil-gap configuration

The steepness of the nonlinear curve directly corresponds with the energy of the higher-order components.

Figure 22 shows the spectrum of the distorted two-tone signal caused by the force factor nonlinearity of the equal-length configuration. Clearly the third-order distortion is maximal and the fifth- and higher-order components rapidly decay. A nonlinearity with a more distinct onset like the *Bl(x)* of an overhang coil produces larger higher-harmonics as shown in Figure 23.

While these spectra are measured at a particular voice coil displacement (x_{peak}= 5mm) it is also interesting to investigate the dependency of the spectrum characteristics on the displacement (which stands for the amplitude of the excitation).
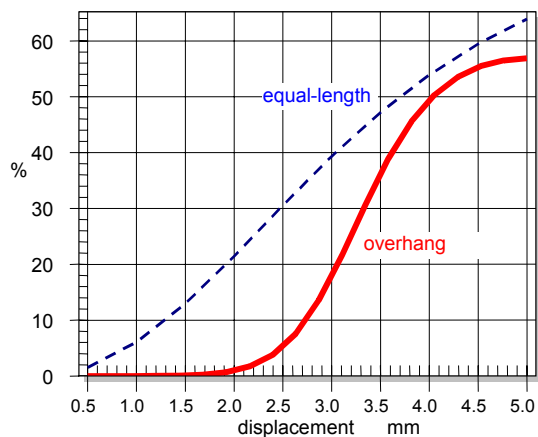
Figure 24: Total harmonic distortion (*THD*) in percent versus voice coil displacement for a motor with an overhang coil (thick line) and with an equal-length configuration (dashed line).

Figure 24 shows total harmonic distortion *(THD)* for both configurations simulated at the resonance frequency versus voice coil displacement x. Since the equal-length configuration causes an early Bl(x) decay, the distortion rises almost linearly with displacement. The equal-length configuration produces 30 % THD at x_{peak}=2.5 mm but the distortion of the overhang coil is about 5 %. At higher displacements the distortion of the overhang coil rises at a much higher rate to almost the same value as the equal-length configuration.
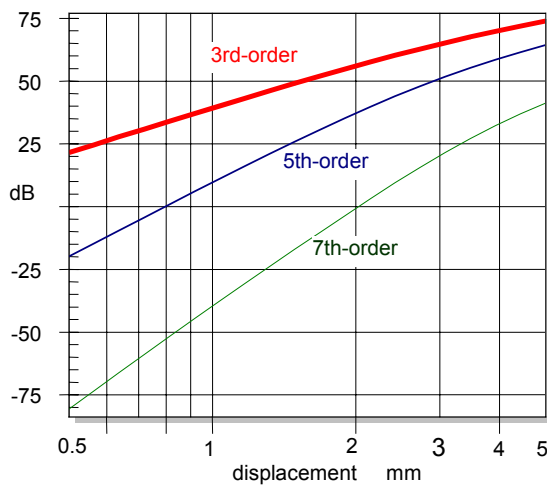
Figure 25: Amplitude of 3rd, 5th and 7th-order harmonic distortion components in sound pressure versus displacement for an equal-length configuration

It is also interesting to investigate the dependency of each distortion component versus displacement. Figure 25 shows the 3rd-,5th- and 7th-order distortion generated by the equal-length configuration versus displacement on a double logarithmic scale. Below 2 mm all the curves are almost perfectly straight lines whose gradient rises with the order of the distortion. This is typical for a weakly nonlinear system with a smooth curve shape (soft nonlinearity). The third-order distortion is below 5 % and the higher-order distortion components are practically negligible. The large signal domain starts at 3 mm where the amplitude compression starts and all of the distortion curves rise at a smaller rate. Due to the feedback loop in the nonlinear differential equation the distortion components reduce the fundamental and disturb their own generation process. Even at 5 mm displacement the 7th-order distortion is 25 dB below the 3rd-order component.
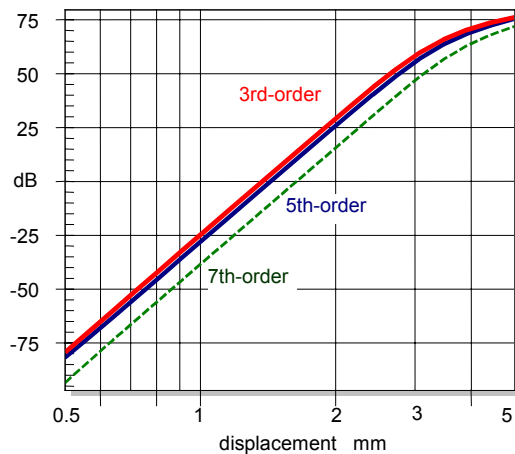
Figure 26: Amplitude of 3rd, 5th and 7th-order distortion components in sound pressure versus displacement for an overhang coil

Figure 26 reveals a completely different behavior of the overhang coil. This behavior is characteristic of a hard-limiting nonlinearity. In the small signal domain all of the curves are also straight lines but now rise at the same rate. Furthermore, low and higher-order components contribute almost the same distortion level. At x_{peak}=3 mm the onset of amplitude compression indicates the large signal domain. Also here the distortion components stay at about the same order of magnitude.

These simulations show pros and cons of the two configurations: The overhang coil clearly gives much less distortion at low and medium amplitude (below the onset point of the hard limiting nonlinearity) while the equal-length configuration (representing a soft limiting nonlinearity) produces low-order distortion at low amplitudes. Operating the loudspeaker in the full large signal range where the coil is half out of the gap, the overhang coil produces higher-order harmonics of larger amplitude than the equal-length coil. Since the higher-order components are located at larger distance from the fundamental components they are less masked by our auditory system and will more likely degrade the subjectively perceived sound quality.
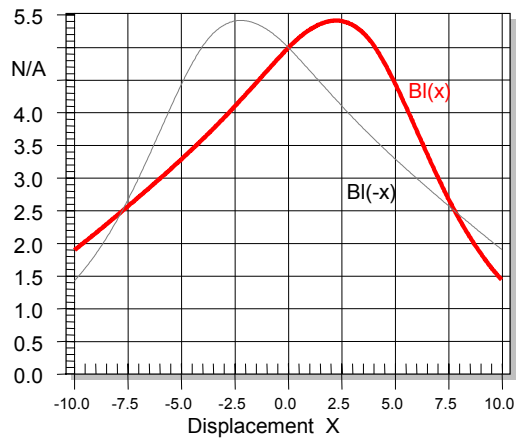
Figure 27: Twisted force factor characteristic

5.3. Twisted Curves

A third graphical feature of the curve shape is the gradual change of the asymmetry causing a twisted curve shape. For example Figure 27 shows a *Bl*-curve which has a distinct maximum at x=2.5 mm. However, the force factor decays at a much higher rate for positive displacement than on the left slope towards negative displacement. Thus, the force factor is lower at a positive displacement of +10 mm than for −10 mm. Such a twisted curve shape has a characteristic effect on the distortion as shown in

Figure 28.
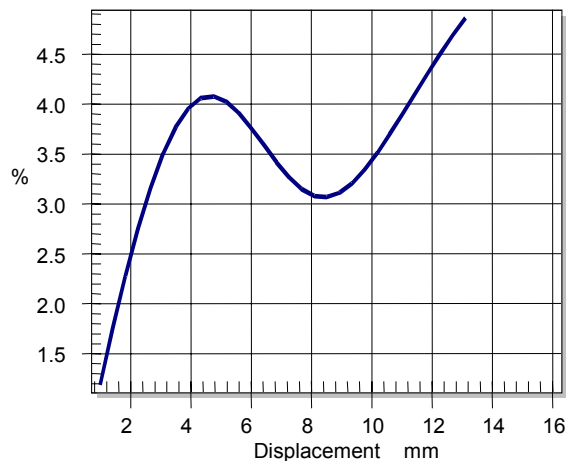
Figure 28: 2nd-order harmonic distortion versus displacement of a motor with asymmetric force factor characteristic as shown in Figure 27.

At small displacements (x < 4 mm peak) the 2nd-order distortion rises with the displacement as expected. The distortion falls for medium amplitudes (4 mm < x < 8 mm peak) and rises again at high amplitudes. Thus, if the direction of the asymmetry varies with displacement some effects can be compensated for. This example also shows that a distortion measurements at one amplitude level can not give a comprehensive description of the large signal behavior.
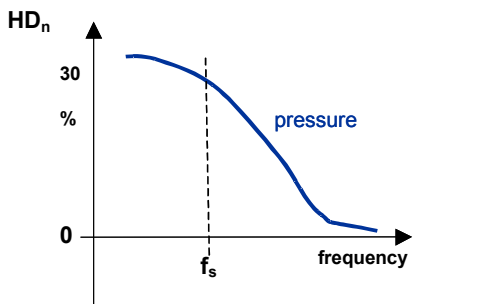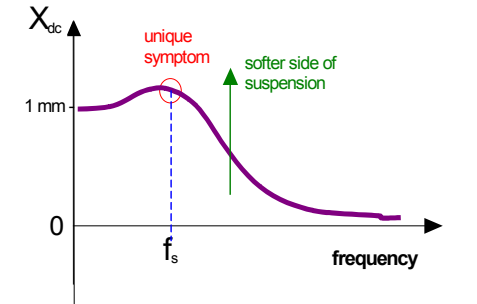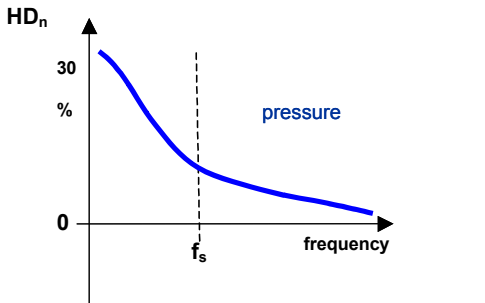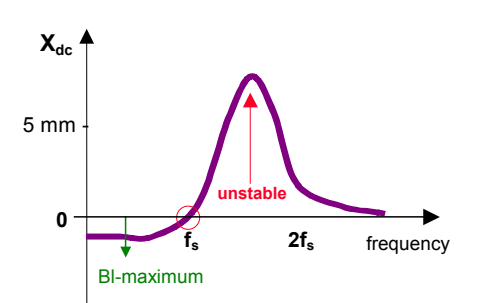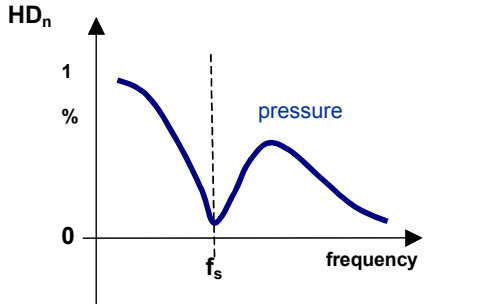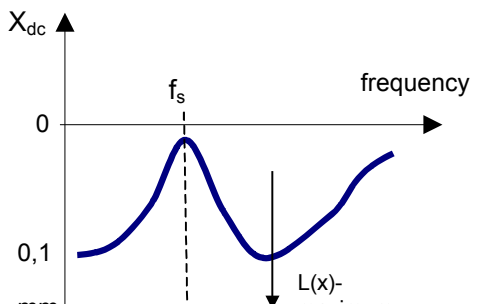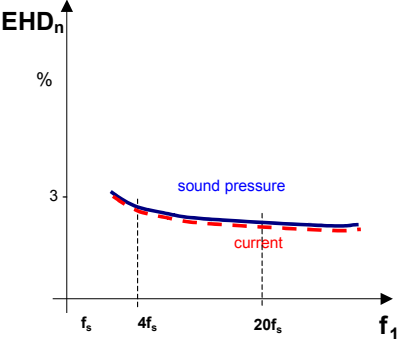
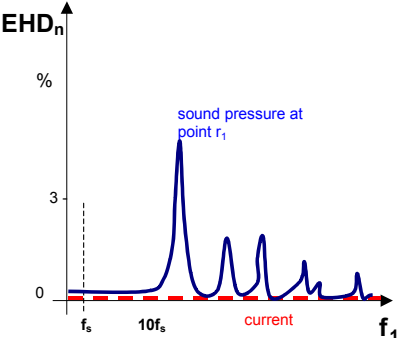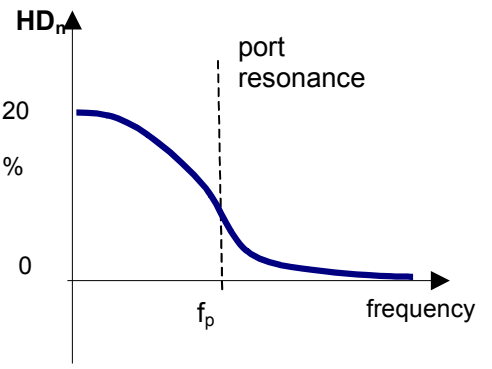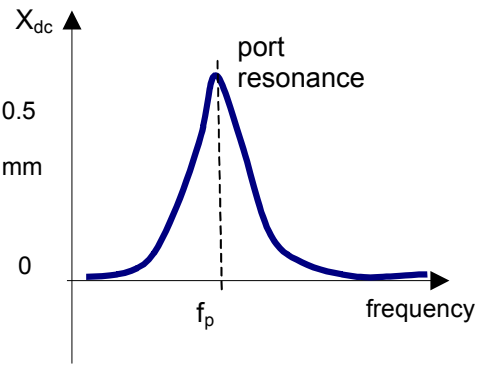## 6.   SYMPTOMS OF LOUDSPEAKER NONLINEARITIES

After discussing the effect of the nonlinear curve shape in general, the physical particularities of the dominant loudspeaker nonlinearities shall be investigated in greater detail. In this section characteristic symptoms for each nonlinearity will be shown. Table 3 anticipates the result of the following discussion. The cross-symbol (X) shows measurements which provide meaningful symptoms for the particular nonlinearity. The star (*) marks unique symptoms which are sufficient to identify the cause of the distortion.

Nonlinearities	SYMPTOMS GENERATED IN MONITORED STATE VARIABLE							
	Sound Pressure				Current			Displacement
	HD	*IMD* (bass sweep)	*IMD* (voice sweep)	*AMD* (voice sweep)	*HD*	*IMD* (bass sweep)	*IMD* (voice sweep)	X_{dc}
$K_{ms}(x)$ suspension (spider +surround)	X							X*
Bl(x) electro-dynamical motor	X	X	X	X				X*
$L_e(x)$ position of coil in the gap		X	X	X		X*	X	
$L_e(i)$ "flux modulation"	X	X	X	X	X*	X*	X	
Geometry of Cone and suspension	X	X	X	X				
Young's-modulus *E(ε)* of cone and suspension	X	X	X	X				
Flow resistance *$R_A(v)$* in ports of vented enclosures	X							
Doppler Effect radiation of sound waves		X	X					
Wave Steepening sound propagation at high SPL	X		X					

* provides unique symptoms which are sufficient for the identification of the nonlinearity.

Table 3 Characteristic symptoms such as harmonic distortion (*HD*), intermodulation distortion (*IMD*), amplitude modulation distortion (*AMD*), dc-displacement (*X_{dc}*) of the dominant loudspeaker nonlinearities (unique symptoms are represented by ☼)

Nonlinearity	Harmonic Distortion	DC Displacement
$K_{ms}(x)$	HD$_n$ — 30% — 0 — pressure — f_s — frequency	X_{dc} — unique symptom — softer side of suspension — 1 mm — 0 — f_s — frequency
$Bl(x)$	HD$_n$ — 30% — 0 — pressure — f_s — frequency	X_{dc} — 5 mm — 0 — unstable — f_s — $2f_s$ — frequency — Bl-maximum
$L_e(x)$	HD$_n$ — 1% — 0 — pressure — f_s — frequency	X_{dc} — f_s — frequency — 0 — 0,1 mm — L(x)-maximum

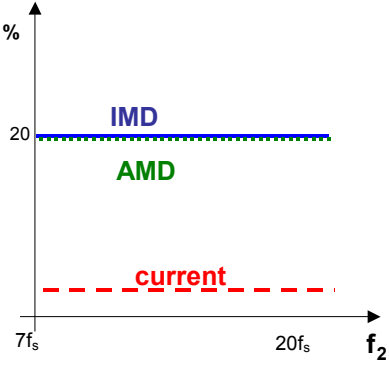| $L_e(i)$		not generated
Variation of Geometry or Young's-modulus $E(\varepsilon)$		not generated
Flow resistance $R_A(v)$ **in ports**		
Doppler Effect	negligible	not generated
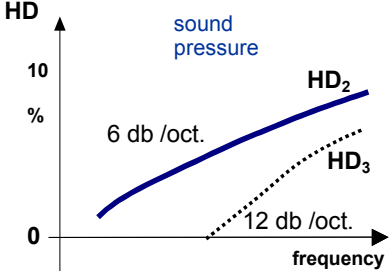
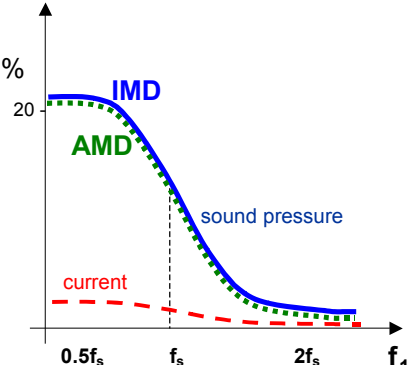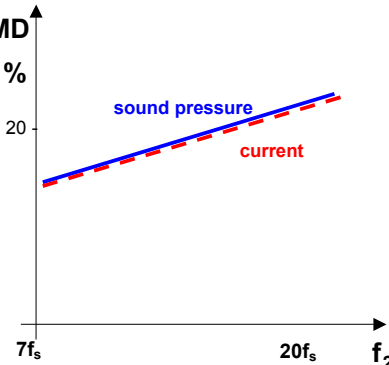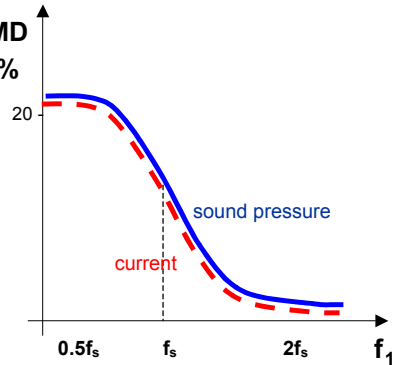| Wave Steepening sound propagation at high SPL | | not generated |

Table 4: Characteristic frequency response of harmonic distortion and dc-displacement.

Nonlinearity	Intermodulation (Voice Tone Sweep)	Intermodulation (Bass Tone Sweep)
$K_{ms}(x)$	negligible	negligible
$Bl(x)$		
$L_e(x)$		

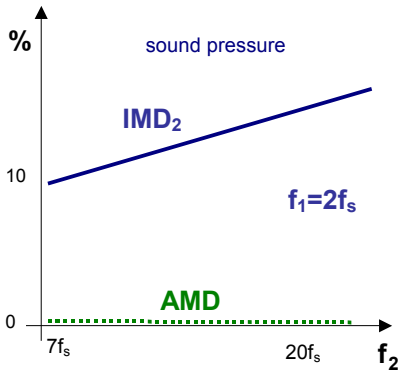|		
$L_e(i)$		
Variation of Geometry and Young's-modulus $E(\varepsilon)$		
Flow resistance $R_A(v)$ in ports	negligible	negligible
Doppler Effect		

41

Wave Steepening sound propagation at high SPL		not applicable

Table 5: Characteristic frequency response of intermodulation distortion.

6.1. Symptoms of $K_{ms}(x)$

Table 1 shows that the restoring force $F=K_{ms}(x)x$ of the suspension is a function of the displacement x only. Since displacement is a low-pass filtered signal, the multiplication of x with x will produce distortion components (both harmonic and intermodulation) which are restricted to low frequencies (for a soft limiting suspension below $5f_s$). A stimulus comprising a low and high frequency tone will not produce significant intermodulation components because the displacement of the high frequency tone is too small. Harmonic distortion measurements provides a sensitive but not unique symptom of the $K_{ms}(x)$-nonlinearity as illustrated in Table 3.

If the $K_{ms}(x)$-curve is asymmetric, the generated dc displacement X_{dc} is a characteristic symptom. Low frequencies which contribute to the ac-displacement contribute to the dc-component as shown in Table 4. The dc-displacement $X_{dc}(f_s)$ at the resonance frequency f_s is a unique symptom for the K_{ms}-nonlinearity. As discussed in greater detail below none of the other dominant nonlinearities can produce a significant dc-component at f_s.

The sign of the dc-part is also a valuable information. The dc-part always moves the coil towards the side where the suspension is softer. If the $K_{ms}(x)$ curve is not twisted the dc-part always has the same polarity and is independent of the amplitude and frequency of the stimulus.

6.2. Symptoms of *Bl(x)*

The *Bl(x)*-nonlinearity causes two effects as shown in Table 1, namely the nonlinear damping and the parametric excitation. Both effects generate high harmonic distortion at low frequencies where displacement, current and velocity are high. The response is almost similar to response caused by the K_{ms}-nonlinearity. Thus the harmonic distortion measurements provide no unique symptoms to distinguish between *Bl(x)* and $K_{ms}(x)$ nonlinearities.

However, the parametric excitation produces high intermodulation distortion in the upper audio band if the first tone provides high displacement and the second tone sufficient current. Table 5 shows a typical *IMD*- response versus frequency f_1 varied at low frequencies ($0.5f_s < f_1 < 2f_s$) while keeping the voice tone at $f_2=10f_s$. The *IMD* components measured in the sound pressure output are significantly higher than in the current signal. Both curves decrease with frequency because the displacement vanishes above resonance.

Table 5 shows typical *IMD* and *AMD* responses measured by using the alternative sweeping technique where the bass tone is at $f_1 = 10$ Hz but the voice tone is varied in the audio band. Since *Bl(x)* produces amplitude modulation both measures give identical values. Both values are also independent of the frequency because the fixed bass tone provides constant peak displacement.

The parametric excitation also generates a dc-displacement if the *Bl(x)*-curve is asymmetrical. However, the sign of the dc-part depends on the phase of current and displacement multiplied with each other and gives the typical response shown in Table 4.

A single tone below resonance also generates a relatively small dc-part which moves the coil towards the *Bl*-maximum. This behavior may partly compensate for an offset in the coil's rest position. The dc-part vanishes at the resonance where current and displacement become 90 degree out of phase. At higher frequencies the self-centering behavior reverses and the coil has the tendency to slide down on either slope of the *Bl(x)*-curve. Even in a perfectly symmetrical *Bl(x)* curve a small disturbance may initiate this coil-jump-out process. This shows that the electro-dynamic transducer is potentially unstable. The dc-force generated by the motor interacts with the stiffness of the suspension at dc. Unfortunately some suspension materials have a significantly lower stiffness at dc than at resonance frequency f_s [24]. Consequently the visco-elastic properties of the suspension material are important for the stability of the motor structure. The zero point of the dc-part ($X_{dc}=0$) at f_s is usually a unique symptom of the *Bl(x)*-nonlinearity. A zero point can only be produced by other nonlinearities ($L_e(x)$ and $K_{ms}(x)$) if the curve is twisted or if the dc-components of two different asymmetrical nonlinearities cancel out each other.

6.3. Symptoms of $L_e(x)$

The $L_e(x)$-nonlinearity supplies distortion directly into the electrical circuit which can easily be detected in the input current. According Table 1 this nonlinearity multiplies current and displacement which are differentiated afterwards.

An $L_e(x)$-nonlinearity produces relatively low harmonic distortion. At low frequencies both current and displacement are high but the differentiator attenuates the harmonics. At the resonance the current is low and at higher frequencies the displacement vanishes.

However, a two-tone signal may activate high intermodulation distortion because the low frequency tone f_1 provides high displacement and the high frequency tone f_2 sufficient current. It is a unique feature of the $L_e(x)$-nonlinearity that the *IMD* detected in the current equals the *IMD* found in the sound pressure output. This is illustrated in Table 5 where the bass tone is varied and the distortion decays above resonance frequency.

Table 5 shows the *IMD* measured with the alternative sweeping technique where the voice tone is varied while keeping the bass tone at a constant frequency. This curve reveals the effect of the differentiator which causes an increase of about 6 dB/octave in the *IMD* and *AMD* response.

The reluctance force generates a unique symptom in the dc-displacement as shown in Table 4. Since the reluctance force is proportional to the squared input current, the force becomes minimal at the resonance frequency f_s. Furthermore, the force and resulting dc-displacement do not change the sign as long as the $L_e(x)$ curve shape is not twisted.

6.4. Symptoms of $L_e(i)$

The variation of the permeability expressed by the current varying inductance $L_e(i)$ causes a multiplication of current signals prior to the differentiation as shown Table 1. The intermodulation distortion measurement with varying bass tone frequency reveals a unique symptom. The *IMD* response has a characteristic minimum at the resonance frequency f_s as shown in Table 5. The *IMD* distortion and the harmonic distortion at higher frequencies measured in sound pressure and current are also identical. Contrary to the displacement varying nonlinarities ($Bl(x)$, $K_{ms}(x)$ and $L_e(x)$) this nonlinearity can also produce significant harmonic distortion (*HD*, *THD*) in both the input current and sound pressure output as shown in Table 4. Single tone harmonic distortion in current and sound pressure are comparable after transforming both results into the equivalent input distortion (EHD).

6.5. Symptoms of varying Cone Geometry

This mechanism is directly related with the occurrence of break-up modes. Thus the distortion components are generated at relatively high frequencies ($>10f_s$). The distortion can easily be measured in the acoustical output but is hardly detectable in the input current. Comparing both measurements may be helpful to separate motor nonlinearities. Maxima in the frequency response of the equivalent harmonic input distortion (*EHID*) corresponds with break-up modes of high amplitude.

Scanning the cone and suspension surface and measuring the distortion directly in the mechanical system would give deeper insight into the nonlinear process.

The intermodulation between a low and high-frequency tone is mostly amplitude modulation. The variation of the surround geometry changes the mechanical impedance at the end of the cone and has significant impact on the amplitude of particular modes.

6.6. Symptoms of nonlinear E-modulus

The variation of the Young's E-modulus produces similar symptoms as those due to variation of the cone and surround geometry. The measurement of harmonic distortion in the sound pressure output gives significant symptoms.

Intermodulation measurements should avoid a low frequency component because a bass tone will cause a significant deformation of the surround geometry which dominates the material nonlinearities.

6.7. Symptoms of the Port Nonlinearity

To evaluate the performance of the port the vented loudspeaker system is excited at the port resonance frequency (Helmholtz resonance) where volume velocity q is maximal but the displacement of the loudspeaker minimal. The harmonic distortion is measured in the sound pressure output at 1 m distance to get a good signal-to-noise ratio. Measurements closer to the port may be affected by air convection. To separate the effect of the port from other loudspeaker nonlinearities the displacement of the cone is also measured by using a laser system. The equivalent harmonic input distortion calculated from the sound pressure signal and the displacement become comparable, and the difference shows the contribution of the port. The third-order harmonic are usually dominant if the port geometry is symmetrical. Measurements of intermodulation distortion will not provide unique symptoms.

6.8. Symptoms of the Doppler Effect

The harmonic distortion measurement is not useful for detecting the Doppler effect. A single signal tone can not provide both sufficient displacement and a short wavelength to produce a significant phase shift. The Doppler effect can be easily detected by performing an intermodulation measurement with a varying voice tone as illustrated in Table 5. Similar to the $L_e(x)$-nonlinearity the intermodulation rises by 6dB per octave to higher frequencies. However, the Doppler effect causes only phase modulation and the value of the amplitude modulation (*AMD*) is low. Clearly the Doppler effect can not produce any distortion in the displacement and in the input current.

6.9. *Symptoms of Wave Steepening*

The nonlinear sound propagation is related to the multiplication of sound pressure components. Thus this nonlinearity produces not only intermodulation but also significant harmonics. This is a unique symptom that distinguishes Doppler effect from wave steeping. The 2nd-order distortion

rises by 6dB per octave while the 3rd-order distortion usually rises at a higher rate because it is generated from the 2nd-order components by an additional multiplication and differentiation in the following horn sections [14] .

7.   PRACTICAL DIAGNOSTICS

The interaction and superposition of the different effects are now discussed on three real loudspeakers:

7.1. Speaker 1 with Coil offset

The first loudspeaker is a 6 inch woofer intended for high quality consumer application. The force factor characteristic *Bl(x)* as shown in Figure 29 reveals a distinct plateau region corresponding with a voice coil overhang of about 6 mm. .
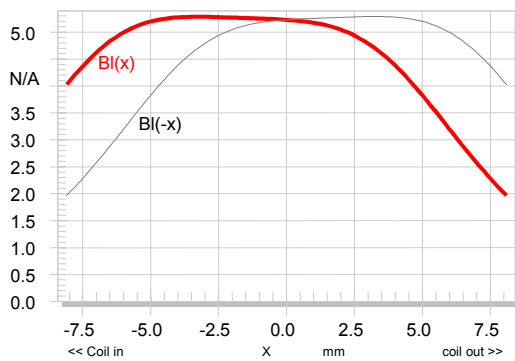
Figure 29: Measured force factor *Bl(x)* versus displacement of speaker 1 (dashed curve shows the mirrored *Bl(-x)*-characteristic)

The optimum rest position of the voice coil can be found by investigating the symmetry of the *Bl*-characteristic in Figure 30. Assuming a sinusoidal displacement of given *amplitude*, the coil will not see the same *Bl*-values at positive and negative peak displacement if the curve is asymmetric. By shifting the coil (*offset)* to the *symmetry point* (red dashed line in Figure 30) the same Bl-values at positive and negative peak values may be accomplished for a particular amplitude. If the symmetry point is independent of the amplitude then the asymmetry can completely be compensated by a constant voice coil shift. However, a compromise may be required as in the example shown in Figure 30 where the symmetry point varies from –3 mm at low amplitudes to –2 mm at higher amplitudes. The *symmetry region* (grey area) shows where a potential offset for a given amplitude generates small asymmetrical variation (< 5 %) which are acceptable. At small amplitudes where the Bl(x)-curve has the plateau, the symmetry region is wide indicating that the position of the overhang coil is not critical here. For larger amplitudes

the voice coil has to be shifted by a negative offset (about -2 mm) that the coil leaves the gap symmetrically.

The rest position of the voice coil in the gap is optimal if the dotted line representing the rest position (offset=0) is in the symmetry region (grey area). If this is not the case the symmetry point gives some indication for a voice coil shift.
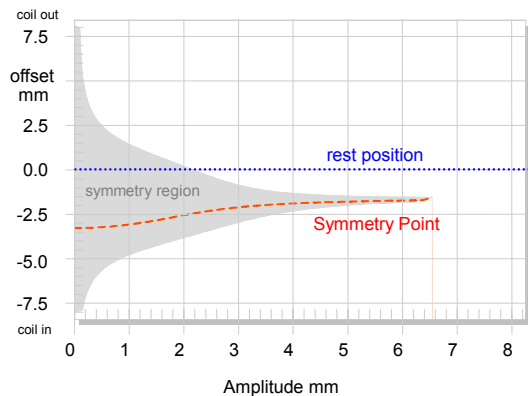

Figure 30: Symmetry point (red dashed line) and symmetry region (grey area) reveal an offset in the coil's rest position of speaker 1.

The stiffness curve shown in Figure 31 has also a small asymmetry and $K_{ms}(x)$ increases for negative excursions to twice the value found at positive values. After removing 80 % of the surround material the measured stiffness of the remaining spider was almost symmetrical.
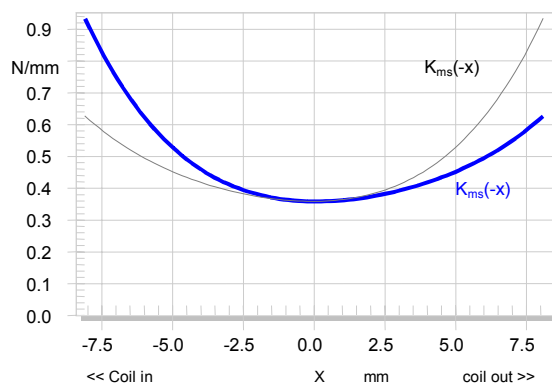
Figure 31: Stiffness $K_{ms}(x)$ versus displacement x of speaker 1 (dashed curve shows mirrored $K_{ms}(-x)$-characteristic)
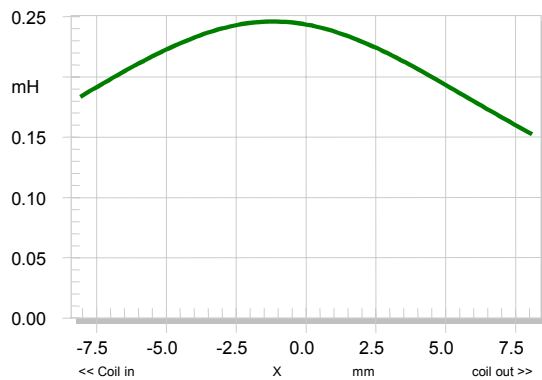
Figure 32: Inductance $L_e(x)$ versus displacement x of speaker 1

Figure 32 shows an almost symmetrical shape of the $L_e(x)$ which is not typical for this type of driver. The missing increase at negative displacement indicates that a shorting ring is used below the gap. The remaining maximum of inductance at $x=0$ may be reduced by placing an additional cap on the pole piece. However, the total inductance value is small (compared with the $R_e= 3.5$ Ohm) and will not produce significant variation of the input impedance.
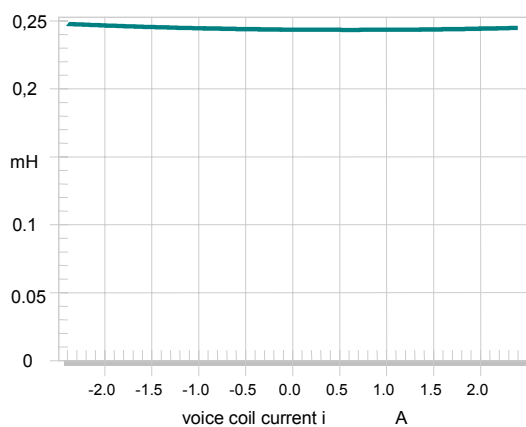
Figure 33: Inductance $L_e(i)$ versus current i of speaker 1

The variation of the voice coil inductance $L_e(i)$ as shown in Figure 33 shows that the permeability of the magnetic path is almost constant. Here the permanent field generated by the magnet is much higher than the ac field generated by the coil.
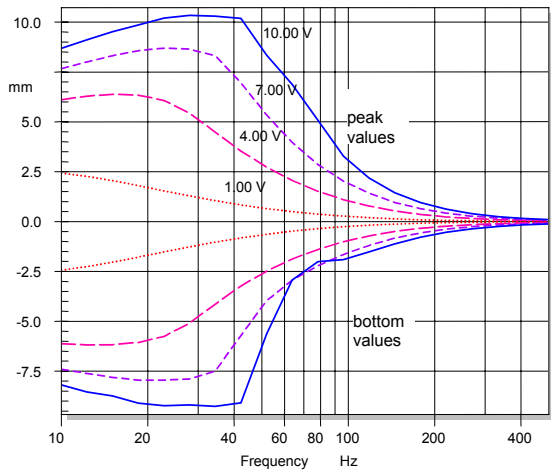
Figure 34: Measured peak and bottom value of voice coil displacement of speaker 1 versus frequency measured at four voltages

Figure 34 shows the peak and bottom of the voice coil displacement measured at four different voltages by a laser displacement meter. The shape of the curves varies with the input voltage. For $U=1V$ the maximum of the displacement is far below resonance due to the high electrical damping and the low total loss factor Q_{ts} of the driver. However, at high voltages the electrical damping decreases (with $1/Bl(x)^2$) and the Q_{ts} becomes greater than 1. At frequencies shortly above resonance the bottom value stagnates at –2.5 mm while the peak values rise rapidly with the input voltage. This corresponds with a dc-part generated in the displacement. This is investigated in Figure 35 in greater detail.
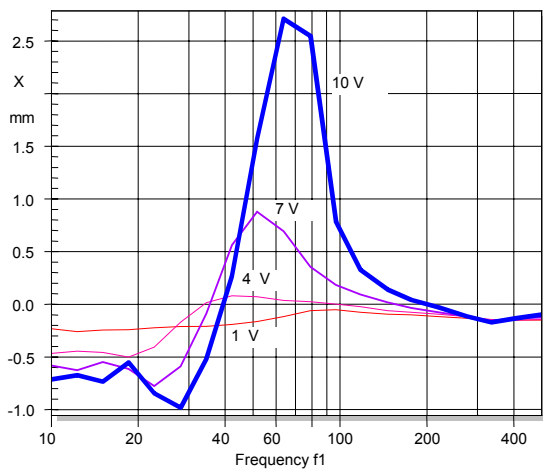

Figure 35: Measured dc-displacement of speaker 1 measured versus frequency and at four voltages

The sign of the dc part changes at the resonance frequency f_s =35 Hz. For frequencies below f_s the dc part is about -0.5 mm and stays almost constant for high amplitudes of the ac signal. Here the asymmetry of $Bl(x)$ generates a dc-force which moves the coil towards the Bl-maximum. At frequencies above f_s the consequences of the voice coil offset become obvious. The dc part becomes positive and rises quickly with amplitude (*coil jump-out effect*). The asymmetry of the stiffness $K_{ms}(x)$ as shown in Figure 31 generates a positive contribution to the dc-part and the inductance $L_e(x)$ a negative dc. However, both parts are negligible in comparison to the dc-part generated by $Bl(x)$.
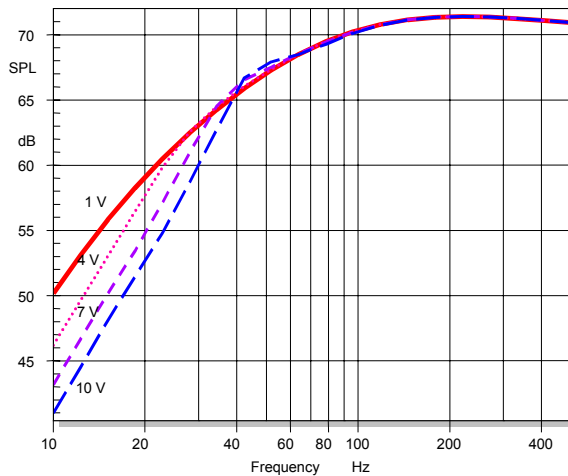

Figure 36: Sound pressure response $P_r(f, U_i)$ measured at four voltages (3 V increments) which are referred to $U_i=1\ V$ to reveal the amplitude compression of the fundamental in speaker 1

Figure 36 shows the frequency response of the fundamental in the sound pressure output measured at four voltages but referred to the measurement in the small signal domain ($U_l=1V$) according Eq. (1). Since the increase of the voltage is compensated this representation shows the power compression directly. At higher frequencies where the displacement becomes small there is no compression and the sensitivity stays constant. If the measurement time would be extended the heating of the coil would cause an additional amplitude compression (thermal effect). At low frequencies the SPL reduces by 8 dB due to the nonlinear effects. At the resonance the vanishing electrical damping causes a negative compression and the loudspeaker produces more output.
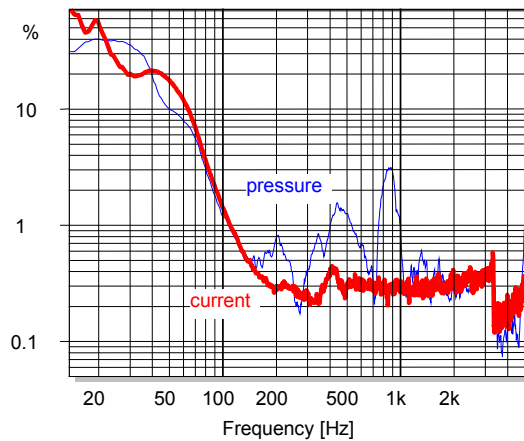
Figure 37: Equivalent total harmonic input distortion (*ETHD*) measured in the sound pressure output (thin curve) and in the voice coil current (thick curve) of speaker 1

The displacement varying force factor *Bl(x)* and stiffness $K_{ms}(x)$ generate high total harmonic distortion in the sound pressure output and in the voice coil current. To compare both signals the concept of equivalent input distortion according Eq. (8) is used. The distortion components measured in sound pressure output and current are transformed to the input (which is a voltage for a normal amplifier with low output impedance) and are presented in Figure 37 as thin and thick curves, respectively. At higher frequencies (*f* > 200 Hz) the distortion components in the current are very low (less than 0.5 %) and are caused by the $L_e(i)$-nonlinearity. The other nonlinearities (*Bl(x)*, $L_e(x)$ and $K_{ms}(x)$) are displacement dependent and can not generate significant harmonic distortion. At particular frequencies e.g. 400 Hz and 800 Hz, nonlinearities in the mechanical domain (cone break-ups) produce additional distortion which interfere with the distortion found in the current. Cancellation of the two distortion components only occurs at 250 Hz but both parts usually increase the total distortion at other frequencies.
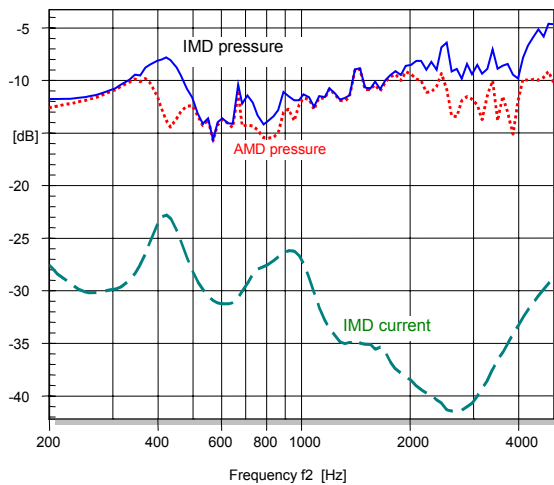
Figure 38: Total intermodulation distortion (IMD_{Total}) of speaker 1 measured in sound pressure and in voice coil current and amplitude modulation distortion (*AMD*) in the sound pressure versus frequency f_2 of the voice tone *(constant bass tone at f_1=10 Hz)*

Figure 38 shows the intermodulation distortion measured with a two-tone stimulus comprising a voice tone with variable frequency f_2 and a bass tone at fixed frequency f_1=10 Hz. The total intermodulation IMD_{total}, measured in the sound pressure output and shown as thin line, are 20 dB higher than the intermodulation found in the input current which are shown as dashed line. Thus the intermodulation components caused by $L_e(x)$ and $L_e(i)$ are almost negligible compared with the contribution of the other nonlinearities.

Figure 38 also shows that the intermodulation distortion components below 2kHz are caused by amplitude modulation (*AM*). For frequencies below 400 Hz the *AMD and IMD*-values are almost constant which is typical for the *Bl(x)*-nonlinearity as illustrated in Table 5. At 400 Hz the cone performs the first partial vibration which is modulated by the varying surround geometry. Above 2 kHz the rising distortion is generated by frequency modulation.
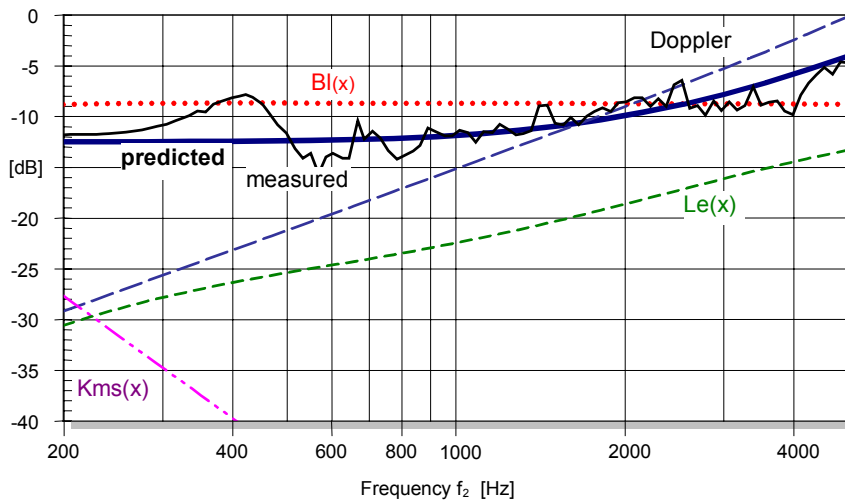
Figure 39: Measured and predicted intermodulation distortion (IMD_{total}) of speaker 1 compared with the contribution of each nonlinearity (sweeping the *voice tone)*

Further insight into the generation of the intermodulation distortion may be gained with use of the simulation tool (SIM2) of the Distortion Analyzer [26] where the total intermodulation can be predicted and the contribution of each nonlinearity can be investigated systematically.

The predicted and measured curves as shown in Figure 39 agree very well. The nonlinear cone vibration is not considered in the model but can easily separated from the motor and suspension nonlinearities. Considering the contribution of the $Bl(x)$ only and switching off all of the remaining nonlinearities ($K_{ms}(x)$=const., $L_e(x,i)$=const., …) the calculated *IMD* distortion is presented as dotted a curve. This curve is constant according to the theoretical shape presented in Table 5 and is the same order of magnitude as the predicted curve considering all nonlinearities. The distortion below 2kHz can be significantly reduced by shifting the rest position of the coil 1.5 mm toward the back-plate. Above 2kHz the Doppler effect becomes dominant and produces significant phase modulation, shown as the dashed line in Table 5. However, phase modulation has less impact on the perceived sound quality than amplitude modulation which is perceived as an unpleasant roughness in the reproduced signal.

The predicted intermodulation generated by $L_e(x)$ corresponds with the small values found in the input current in Figure 38 .

The low *IMD* values of the stiffness $K_{ms}(x)$ correspond with Table 3 showing that intermodulation distortion is not a significant symptom of the suspension nonlinearity.
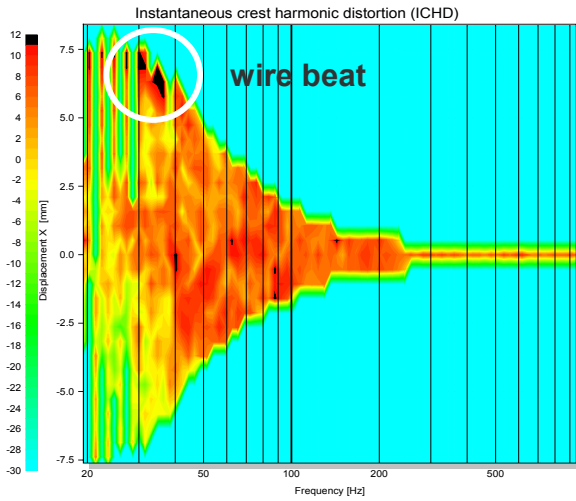
Figure 40: Measured instantaneous crest factor of harmonic distortion (color coded) plotted versus frequency and voice coil displacement

Finally the loudspeaker is checked for transient and impulsive distortion which have a high peak value but a relatively low *rms*-value. Figure 40 shows the instantaneous crest factor *ICHD* which is coded by the color and displayed versus frequency (x-axis) and displacement (y-axis). Below 7 mm the crest factor of harmonic distortion is less than 10 dB (blue to red) which is typical for regular nonlinearities in the motor, suspension or cone. However, at high positive displacement occurring at low frequencies (f < 40 Hz) the crest factor exceeds 10 dB (becoming black) which indicates a nonlinear mechanism producing short clicks at the particular coil position. Further examination of the driver revealed that the flex wires hit the cone at this point.

7.2. Speaker with Suspension problem

Loudspeaker 2 is a 5 inch woofer which is also intended for consumer application.

Figure 41: Force factor *Bl(x)* versus displacement of speaker 2 (thin curve shows mirrored *Bl(-x)*-characteristic)

The force factor *Bl(x)* shown in Figure 41 is relatively linear by using a high coil overhang. The curve has no plateau but a gradual decay because the fringe field outside the gap is much higher than in speaker 1.
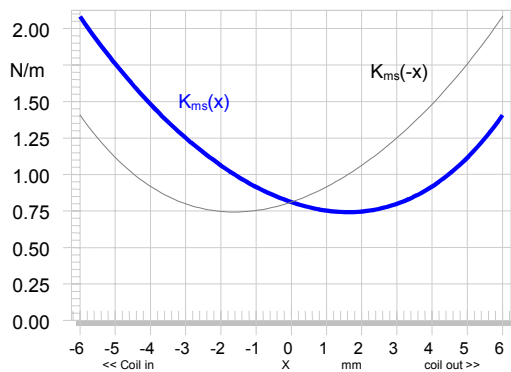

Figure 42: Stiffness $K_{ms}(x)$ versus displacement x of speaker 2 (thin curve shows mirrored $K_{ms}(-x)$-characteristic)

The stiffness curve in Figure 42 has a severe asymmetry. This is shown to be by the spider because a similar curve is found in a second measurement after removing 80 % of the surround material.
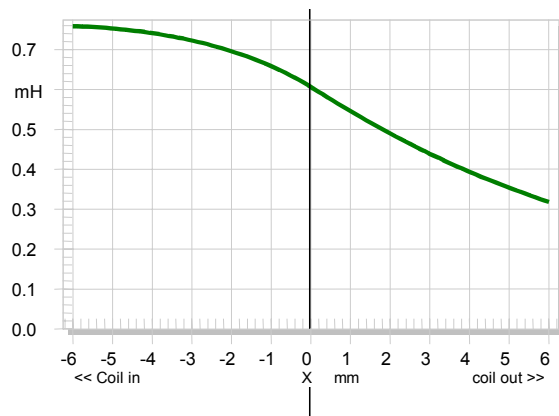
Figure 43: Inductance $L_e(x)$ versus displacement x of speaker 2

The inductance $L_e(x)$ is also asymmetric and rises for negative excursion of the coil to the back-plate. This is typical for a motor without any shorting material. While the inductance $L_e(x)$ versus displacement varies by 100 % the inductance $L_e(i)$ versus input current i in Figure 44 varies only by 10 %.
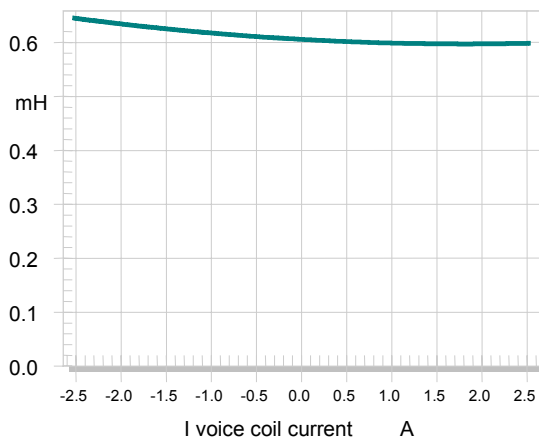

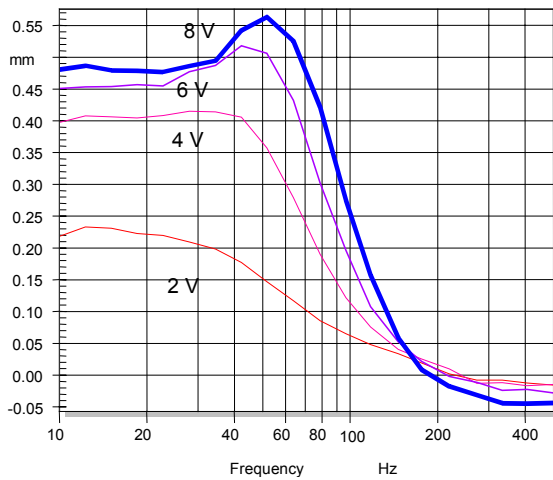Figure 44: Inductance $L_e(i)$ versus current i of loudspeaker 2

Figure 45: Measured dc-displacement versus frequency measured at four different voltages of loudspeaker 2

The measured dc-displacement as shown in Figure 45 agrees with the asymmetries found in the nonlinear parameters. The asymmetric stiffness generates a positive displacement because the suspension is much softer for positive than negative displacement. The dc-displacement becomes maximal at the resonance frequency where the amplitude of the current is minimal and the other nonlinearities give a smaller contribution to the dc-part. At higher frequencies the stiffness asymmetry can not produce a significant dc-part because the displacement is small. Only the reluctance force generates a small negative dc-displacement in this frequency range and moves the coil in a negative direction where the inductance $L_e(x)$ becomes higher.
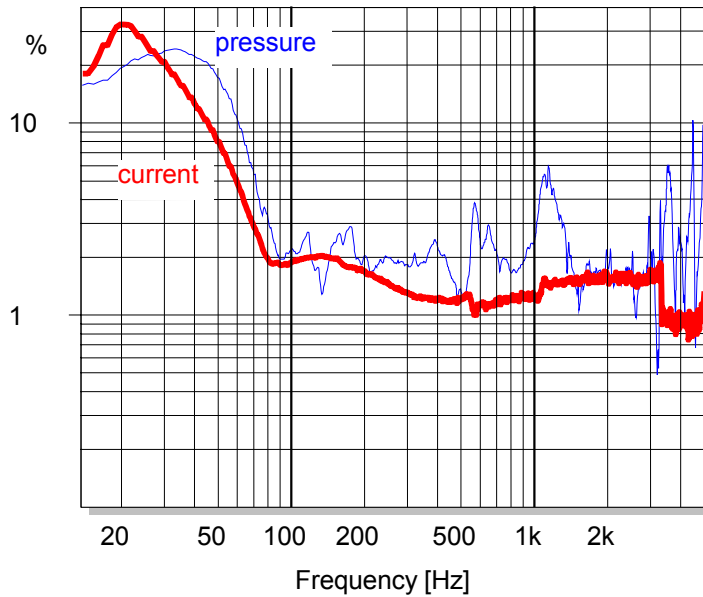
Figure 46: Equivalent total harmonic input distortion *(ETHD)* measured in the sound pressure output (thin curve) and in the voice coil current (thick curve) of loudspeaker 2

Figure 46 compares the harmonic distortion found in the input current and in the sound pressure output. At the resonance frequency and below, most of the harmonic distortion found in current and sound pressure is caused by the nonlinear suspension. For frequencies above 80 Hz the nonlinear inductance $L_e(i)$ of Figure 44 generates 1 .. 2 % in the input current. The distortion measured in the sound pressure response show contributions from the other displacement varying nonlinearities (*Bl(x)*, *$L_e(x)$* and *$K_{ms}(x)$)* below 1000 Hz and interferences from nonlinear cone vibration at higher frequencies.
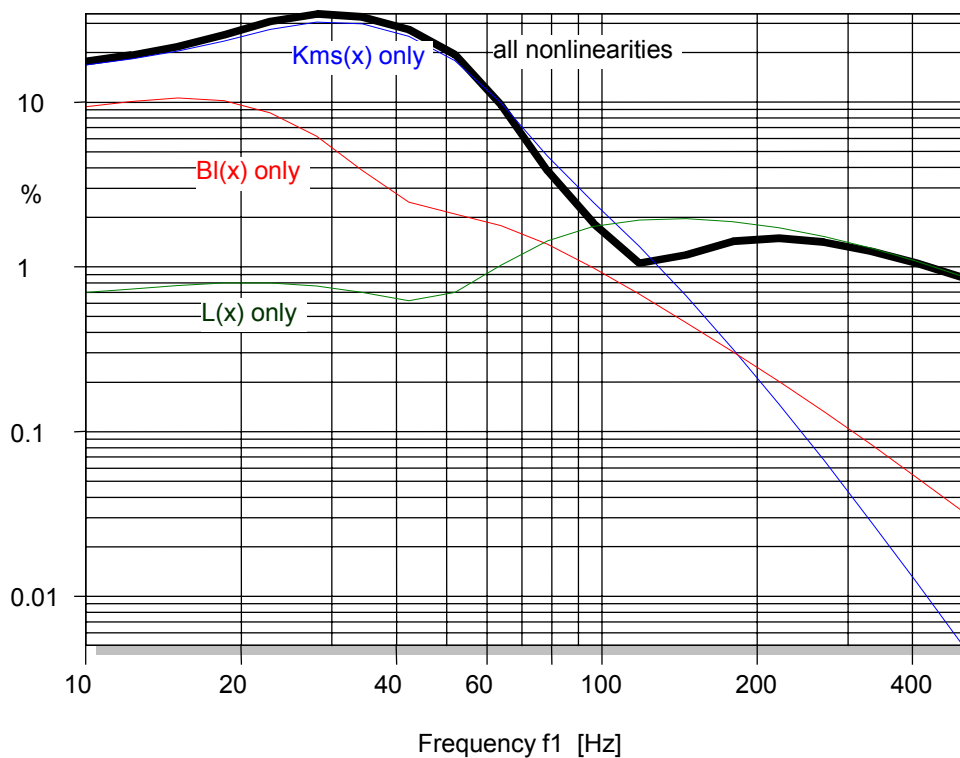
Figure 47: Equivalent total harmonic input distortion predicted by using all nonlinearities (solid curve) and in the sound pressure output (thin curve) and in the voice coil current (thick curve) of loudspeaker 2.

The identified nonlinear parameters allow one to investigate the contribution of each nonlinearity in greater detail. Figure 47 shows that the stiffness $K_{ms}(x)$ is the dominant cause for the *ETHD*. The force factor *Bl(x)* produces only 10 % distortion and the inductance $L_e(x)$ produces 1 -2 %.
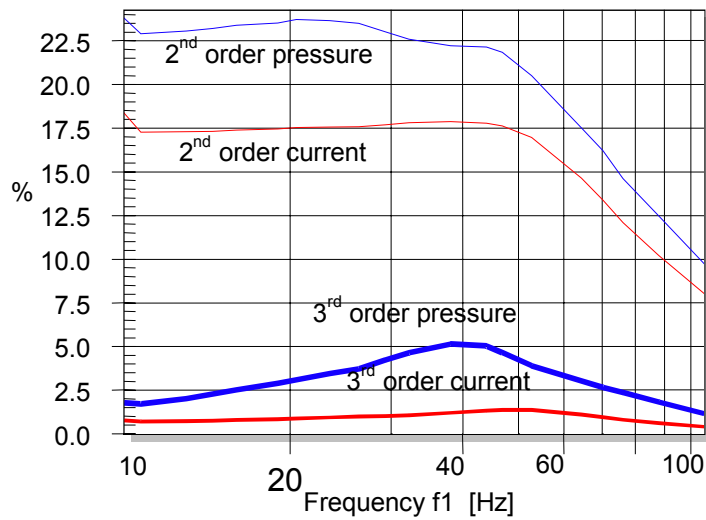
Figure 48: 2nd-order and 3rd-order intermodulation distortion measured in voice coil current and sound pressure output of loudspeaker 2 (varying bass tone, f_2=500 Hz)

Figure 48 reveals high 2nd-order intermodulation distortion $IMD_2 \approx 20$ %. This is caused by the $L_e(x)$-nonlinearity because almost the same values are found in the current and pressure signals and there is no dip at resonance frequency f_s. Due to the asymmetrical shape of $L_e(x)$ the 2nd-order component IMD_2 is much higher than the 3rd-order component IMD_3.

7.3. Loudspeaker 3 with flux modulation

Loudspeaker 3 is a 12 inch speaker intended for automotive application. Figure 49 reveals a very symmetrical $Bl(x)$ characteristic which is almost constant up to 15 mm peak value.
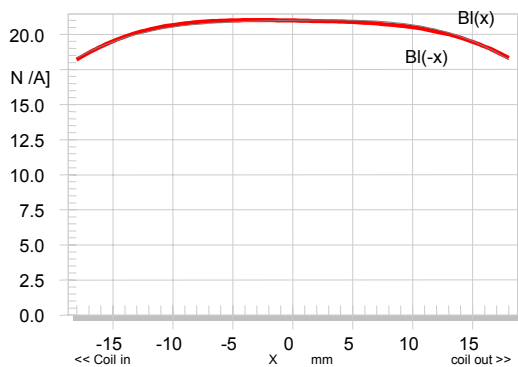
Figure 49: Force factor *Bl(x)* versus displacement of loudspeaker 3 (thin curve shows mirrored *Bl(-x)*-characteristic)
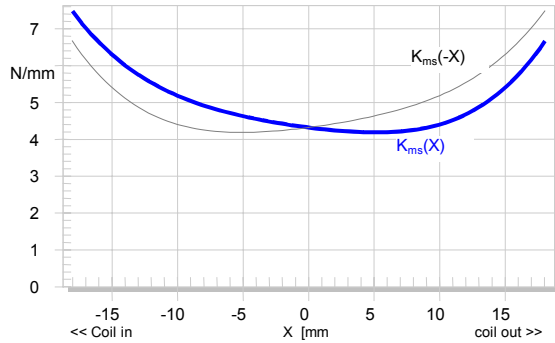
Figure 50: Stiffness $K_{ms}(x)$ versus displacement x of loudspeaker 3 (thin curve shows mirrored $K_{ms}(-x)$-characteristic)

The stiffness $K_{ms}(x)$ of the suspension as shown in Figure 50 is also almost symmetrical. The surround made of thick rubber material causes a minor asymmetry. However, the voice coil inductance varies significantly with displacement and current as shown in Figure 51 and Figure 52, respectively.
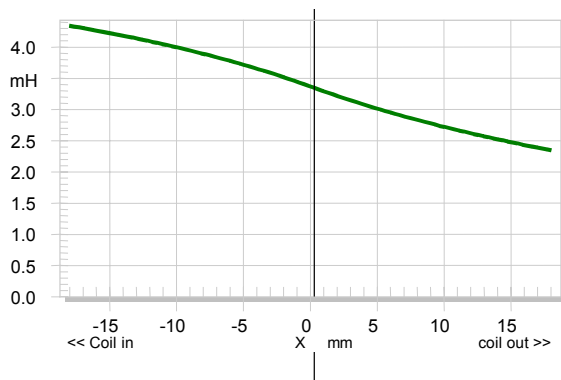
Figure 51: Inductance $L_e(x)$ versus displacement *x* of loudspeaker 3
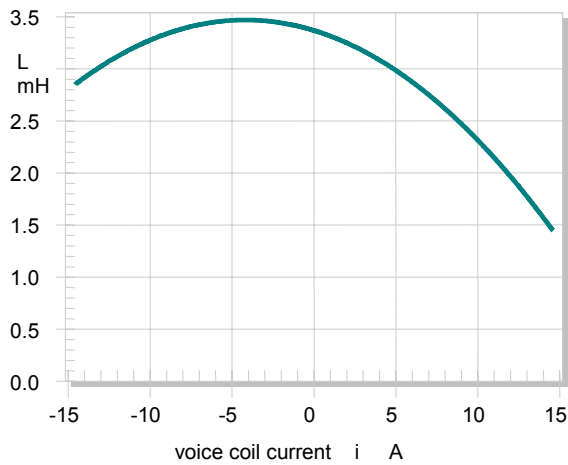
Figure 52: Inductance $L_e(i)$ versus current i of loudspeaker 3

The asymmetrical shape is typical for a motor without any shorting material. The 3.5 mH inductance dominates the electrical input impedance at higher frequencies. During the large signal parameter measurement (LSI) the peak value of current and displacement exceeded 15 ampere and 18 mm, respectively, which caused significant variations of electrical input impedance at higher frequencies. The $L_e(x)$ is more asymmetric than the $L_e(i)$ characteristic.

Figure 53: dc-displacement versus frequency measured (dotted line) and predicted by considering all nonlinearities (thick line) and the contribution of each nonlinearity $Bl(x)$, $K_{ms}(x)$ and $L_e(x)$ of loudspeaker 3

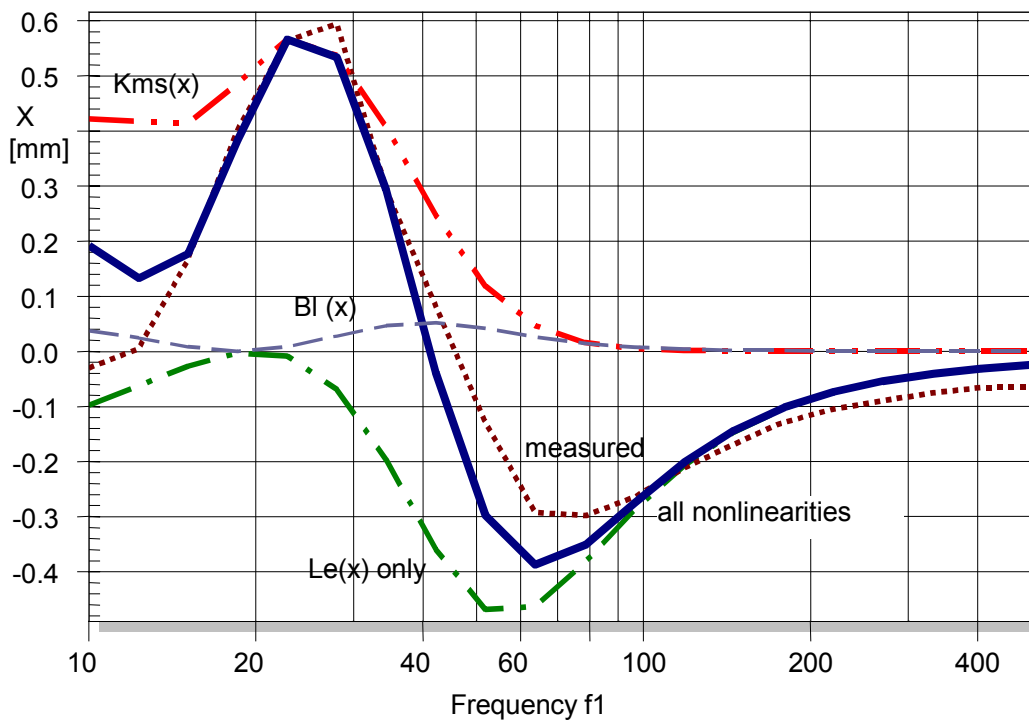Figure 53 shows the frequency response of the dc-displacement measured by a sensor and predicted by using the large signal parameters in the simulation software (SIM) [25]). At the resonance frequency of 25 Hz the positive dc-part of 0.6 mm is caused by the suspension which is softer for positive than for negative displacement as shown in Figure 50. The symmetrical $Bl(x)$-characteristic generates almost no dc-part. However, the asymmetric inductance $L_e(x)$ in Figure 51 generates a negative dc-part below and above f_s. At very low frequencies (10 Hz) the negative dc part of the inductance reduces the positive dc-part generated by the suspension. At higher frequencies (80 Hz) where the current becomes high again but the displacement is small the reluctance force dominates the total dc-displacement. The zero point ($X_{dc}=0$) at 50 Hz is not generated by an asymmetric $Bl(x)$ but is caused by the interaction of two asymmetrical nonlinearities.
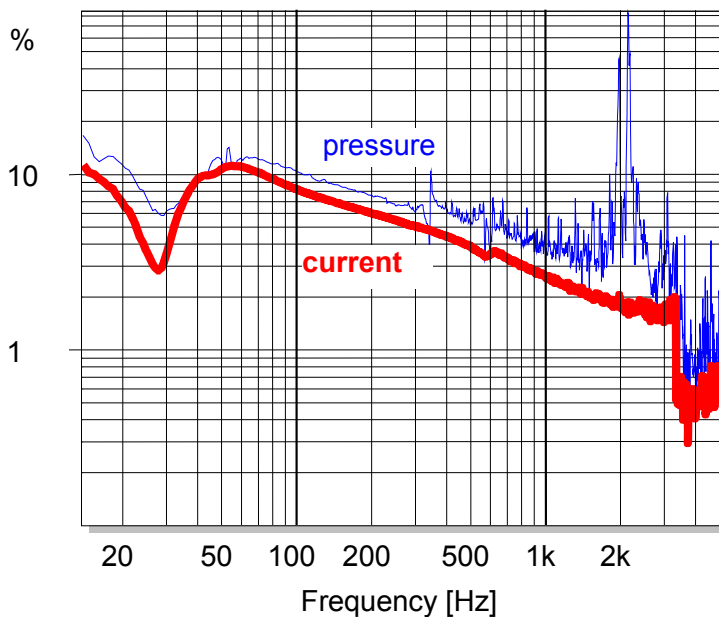
Figure 54: Equivalent total harmonic input distortion (*ETHD*) measured in the sound pressure output (thin curve) and in the voice coil current (thick curve) of loudspeaker 3

The total harmonic distortion measured in sound pressure output and current input are presented as equivalent input distortion *ETHD* in Figure 54. The high inductance nonlinearity $L_e(i)$ generates high distortion in the input current (10% at 50 Hz) which dominates the sound

pressure output. At 2 kHz the cone exhibits nonlinear vibration but this frequency is far beyond the intended working range of the automotive subwoofer.
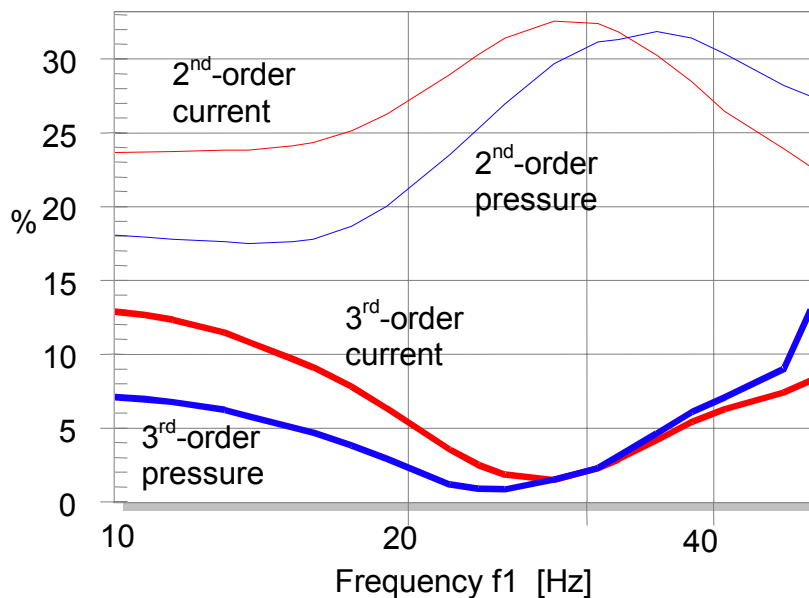

Figure 55: 2nd-order and 3rd-order intermodulation *IMD* in measured in voice coil current and sound pressure output of loudspeaker 3 (varied bass tone, f_2= 300 Hz)

The intermodulation between a variable frequency bass tone at f_1 and the fixed voice tone at frequency f_2= 300 Hz is shown in Figure 55. Like the harmonic distortion, the intermodulation in the current and sound pressure output is of the same order of magnitude. According to Table 3 this is a characteristic symptom of both inductance nonlinearities $L_e(x)$ and $L_e(i)$. The 2nd-order intermodulation IMD_2 has a maximum at the resonance frequency which is typical for $L_e(x)$-nonlinearity varying with displacement. The 3rd-order distortion IMD_3 has a dip at the resonance frequency f_s which is the characteristic symptom for the $L_e(i)$-nonlinearity because the current becomes minimal there.

Loudspeaker 3 is an example of a speaker which is optimized for linear *Bl(x)* and $K_{ms}(x)$ characteristic by using a long voice coil, a carefully designed magnetic path and a two-spider suspension. Despite the development effort, final cost and weight of the product the driver produces a highly distorted output due to the neglected $L_e(x)$ and $L_e(i)$-nonlinearities. Applying some means for shorting the ac-field can improve loudspeaker 3 significantly.

8. CONCLUSION

In the last 20 years significant progress has been made in understanding the large signal behavior of loudspeakers.

Reliable models have been developed for displacement and current varying nonlinearities in the motor and suspension system. The nonlinear parameters $Bl(x)$, $L_e(x)$, $K_{ms}(x)$ and $L_e(i)$ can be measured dynamically on loudspeakers, headphones, micro-speakers and other transducers, with and without enclosure. Finite element analysis (FEA) can also be used to simulate those parameters from geometry and material parameters. The large signal model and the identified parameters allow numerical prediction of the nonlinear symptoms with high precision.

This opens the way for a new kind of loudspeaker diagnostic:

- The nonlinear parameters are easy to interpret and reveal the physical causes almost directly.

- The effect of each nonlinearity can be investigated separately and the causes for signal distortion, instabilities, compression and other nonlinear symptoms can be found.

- Design choices can easily be evaluated and the loudspeaker optimized with respect to size, weight, cost and performance

The knowledge from theory and practical application gives new insight into the general distortion measurements and shows how to make such measurements more comprehensive, time-effective, critical and easier to interpret. The most important points are:

- Nonlinear distortion measurements should be performed at different amplitude levels.

- Harmonic distortion measurements assess particular symptoms (HD_n, *THD, EID, ICHD,* …) of the loudspeaker. However, using a single tone as stimulus is not sufficient to describe the large signal performance comprehensively and to identify all loudspeaker nonlinearities.

- The stimulus should contains at least two tones at the same time to measure intermodulation distortion products which are generated by the multiplication of two different state signals (e.g. displacement and current). The frequency of the tones and the sweeping techniques are critical to get results which are easy to explain. The paper suggests two techniques (sweeping the bass or the voice tone while keeping the other tone at a constant frequency).

- The dc-displacement is a very informative symptom. It gives unique clues to identify the particular causes and to estimate the asymmetry of motor and suspension nonlinearities.

- The amplitude compression of the fundamental and distortion components is also a symptom of loudspeaker nonlinearities. However, it gives no detailed information as to the physical cause.

- The calculation of Equivalent Input Distortion (EID) is a very useful way of post-processing the measured distortion. It suppresses the influence of the linear transfer path (mechanical vibration, radiation, propagation, room, sensor) and simplifies the interpretation of the distortion responses. In this way distortion measured in displacement, current and sound pressure can easily be compared. This gives valuable clues for separating motor- and cone nonlinearities.

- Measurements of the distortion in the sound pressure output should be performed in the near field of the loudspeaker where the signal-to-noise ratio is high. After calculating the equivalent input distortion the distortion at any point in the sound field can easily be predicted by using the linear transfer function measured at lower amplitudes.

- The distortion in the input current gives valuable information about the motor nonlinearities.

- The crest factor of harmonic distortion (*ICHD*) describes the smoothness of the nonlinearity. It exploits the phase information of higher-order harmonics and indicates transient, impulsive distortion caused by loudspeaker defects (e.g. rub & buzz) or extremely hard limiting nonlinearities.

These conclusions lead to a suite of objective measurements which can be accomplished in a few minutes. These measurements give a much more comprehensive picture of the large signal performance than a traditional harmonic distortion measurement. The results can be summarized in a small set of data which is easy to interpret as demonstrated on three loudspeaker examples in this paper. Tables 1 - 5, give a short summary on the dominant nonlinearities and characteristic symptoms which may be helpful to apply this knowledge in daily work.

9.   REFERENCES

[1] A. J. M. Kaizer, "Modeling of the Nonlinear Response of an Electrodynamic Loudspeaker by a Volterra Series Expansion," *J. Audio Eng. Soc.*, vol. 35, pp. 421-433 (1987 June).

[2] J. Vanderkooy, "A Model of Loudspeaker Driver Impedance Incorporating Eddy Currents in the Pole Structure," J. Audio Eng. Soc., Vol. 37, No. 3, pp. 119-128, March 1989.

[3] W. M. Leach, "Loudspeaker Voice-Coil Inductance Losses: Circuit Models, Parameter Estimation, and Effect on Frequency Response, " J. Audio Eng. Soc., Vol. 50, No. 6, pp. 442-450, June 2002.

[4] J.R. Wright, "An Empirical Model for Loudspeaker Motor Impedance, "

J. Audio Eng. Soc. Vol. 38, No. 10, pp. 749-754, October 1990.

[5] M. Dodd, et. al., "Voice Coil Impedance as a Function of Frequency and Displacement" presented at the 117th Convention of the Audio Eng. Soc. , 2004 October 28–31, San Francisco, CA, USA.

[6] A. Chaigne, "Influence of Material and Shape on Sound Reproduction by an Electrodynamic Loudspeaker," presented at the 118th Convention of the Audio Eng. Soc. , 2005 May 28–31, Barcelona, Spain, preprint 6420.

[7] O. Thomas, "Analyse et modelisation de vibrations non-lineaires de milieux minces elastiques," These of UPMC (Paris 6), (2001 October).

[8] J. Vanderkooy, "Nonlinearities in Loudspeaker Ports," presented at the 104th Convention of the Audio Eng. Soc., 1998 May 16 – 19, Amsterdam, NL, preprint 4748.

[9] N.B. Roozen, "Reduction of Bass-Reflex Port Nonlinearities by Optimizing the Port Geometry," presented at the 104th Convention of the Audio Eng. Soc., 1998 May 16 – 19, Amsterdam, NL, preprint 4661.

[10] P. Merkli, et. al., " Transition to turbulence in oscillating pipe flow," J. Fluid Mech. 68 (3), 567 – 575 (1975).

[11] B. Zoltogorski, "Moving Boundary Condition and Non-Linear Propagation as the Sources of Non-Linear Distortion in Loudspeaker," presented at the 94th Convention of the Audio Eng. Soc., 1993 March 16-19, Berlin Germany, preprint 3510.

[12] H. J. Butterweck, "About the Doppler Effect in Acoustic Radiation from Loudspeakers," Acustica Vol. 63, pp. 77 –79, (1987).

[13] L. J. Black, "A Physical Analysis of Distortion produced by the Nonlinearity of the Medium," J. Acoust. Soc. Am. 1, 266 – 267 (1940).

[14] W. Klippel, "Nonlinear Wave Propagation in Horns and Ducts," J. Acoust. Soc. Am. vol. 98, No. 1 , 431 – 438 (July 1995).

[15] E. Czerwinski, "Air-Related Harmonic and Intermodulation Distortion in Large Sound Systems," J. Audio Eng. Soc., vol. 47, No. 6, pp. 427-446, June 1999.

[16] W. Klippel, "Modeling the Nonlinearities in Horn Loudspeakers," J. Audio Eng. Society, vol. 44, pp. 470-480 (1996).

[17] S. Temme, et. al., "Loose Particle Detection in Loudspeakers," presented at the 115th Convention of the Audio Eng. Soc., September 2003, preprint 5883.

[18] W. Klippel, et. al. , "Loudspeaker Testing at the Production Line," presented at the 120th Convention of the Audio Eng. Soc., Paris (France), September 2006, May 20-23, preprint 6845.

[19] "Sound System Equipment – Electroacoustical Transducers – Measurement of Large Signal Parameters," IEC Publication PAS 62458 © IEC:2006(E).

[20] D. Clark, "Precision Measurement of Loudspeaker Parameters," J. Audio Eng. Soc. vol. 45, pp. 129 – 140, (1997 March).

[21] R. H. Small, "Assessment of Nonlinearity in Loudspeakers Motors," in IREECON Int. Convention Digest (1979 Aug.), pp. 78-80.

[22] W. Klippel, "Measurement of Large-Signal Parameters of Electrodynamic Transducer," presented at the 107th Convention of the Audio Engineering Society, New York, September 24-27, 1999, preprint 5008.

[23] M. Knudsen, et. al., "Determination of Loudspeaker Driver parameters Using a System Identification Technique," ," *J. Audio Eng. Soc*. vol. 37, No. 9.

[24] M.H. Knudsen et. al., "Low-Frequency Loudspeaker Models that Include Suspension Creep*," J. Audio Eng. Soc*., vol. 41, pp. 3-18, (Jan./Feb. 1993).

[25] Specification of the KLIPPEL Analyzer System, Klippel GmbH, www.klippel.de, 2005.

[26] W. Klippel, "Prediction of Speaker Performance at High Amplitudes," presented at 111th Convention of the Audio Engineering Society, 2001 September 21–24, New York, NY, USA.

[27] W. Klippel, "Speaker Auralization – Subjective Evaluation of Nonlinear Distortion," presented at the 110th Convention of the Audio Engineering Society, Amsterdam, May 12-15, 2001, preprint 5310, J. Audio Eng. Society, Vol. 49, No. 6, 2001 June, P. 526.

[28] A. Voishvillo, "Graphing, Interpretation, and Comparison of Results of Loudspeaker Nonlinear Distortion Measurements," J. Audio Eng. Society, Volume 52, Number 4, pp. 332-357, April 2004.

[29] A. Dobrucki,   "Nontypical Effects in an Electrodynamic Loudspeaker with a Nonhomogeneous Magnetic Field in the Air Gap and Nonlinear Suspension," *J. Audio Eng. Soc.,* vol. 42, pp. 565 - 576, (July./Aug. 1994).

[30] J.W. Noris, "Nonlinear Dynamical Behavior of a Moving Voice Coil," presented at the 105th Convention of the Audio Engineering Society, San Francisco, September 26-29, 1998, preprint 4785.

[31] "Sound System Equipment. Part 5: Loudspeakers," IEC Publication 60268-5.

[32] S. F. Temme, "How to Graph Distortion Measurements, " presented at the 94th Convention of Audio Eng. Soc. , 1993 March 16-19, Berlin, preprint 3602.

[33] W. Klippel, "Equivalent Input Distortion," J. Audio Eng. Society **52**, No. 9 pp. 931-947 (2004 Sept.).

[34] W. Klippel, „Measurement of Impulsive Distortion, Rub and Buzz and other Disturbances", presented at the 114th Convention of the Audio Engineering Society, 2003 March 22–25, Amsterdam, The Netherlands, preprint # 5734.

[35] D. Clark, "Amplitude Modulation Method for Measuring Linear Excursion of Loudspeakers," presented at the 89th Convention of the Audio Eng. Soc., J. Audio Eng. Soc. (Abstracts), vol. 38, p. 874 (1990 Nov.), preprint 2986.

[36] R. H. Small, "Measurement of Loudspeaker Amplitude Modulation Distortion," presented at the 114th Convention of the Audio Eng. Soc. in Amsterdam, March 22 – 25, 2003, preprint 5731.

[37] W. Klippel, "Nonlinear Large-Signal Behavior of Electrodynamic Loudspeakers at Low Frequencies," *J. Audio Eng. Soc*. , vol. 40, pp. 483-496 (1992).

[38] E. Czerwinski, et. al., "Multitone Testing of Sound System Components – Some Results and Conclusions, J. Audio Eng. Soc. vol. 49, pp. 1011 - 1048 (2001 Nov.).

[39] W. Klippel, "Assessment of Voice-Coil Peak Displacement X_{max}," J. Audio Eng. Society **51**, vol. 5, pp. 307 - 323 (2003 May).